NTNU – Trondheim
Norwegian University of
Science and Technology

Core-Shell nanoparticles as drug delivery vehicles

Manuel Canelas

Chemical Engineering
Submission date: June 2014
Supervisor: Wilhelm Robert Glomm, IKP
Co-supervisor: Sulalit Bandyopadhyay, IKP

Norwegian University of Science and Technology
Department of Chemical Engineering

Table of Contents

Abstract

Targeted drug delivery, magnetic resonance imaging (MRI), diagnosis and treatment of diseases are just a few examples of the wide range of applications of polymer metal nano-particle (NP) hybrids. The field has received further impetus when it comes to controlled release of drug in response to external stimulus.

The current project has investigated the synthesis and characterization of Fe@Ag NPs followed by their functionalization, with an aim to study the loading efficiency and release kinetics of a standard drug, paracetamol. Spherical Fe@Ag NPs with an average diameter of 39nm have been synthesized using a solution based synthetic route, employing heterogeneous nucleation on pre-synthesized Fe core NPs. These NPs were functionalized using functional polymers (PNIPAM and Poly Lysine) and a carrier protein, BSA (Bovine serum albumin) and thereafter used to study paracetamol loading. The loading efficiency was optimized with respect to particle concentration and drug concentration, achieving upto 8% of loading eeficiency. In order to further enhance the loading efficiency, modified BSA nanoclusters were used. A loading efficiency of upto 6% was achieved and to ascertain high loading efficiencies, a complete matrix of parameters needs to be comprehensively studied.

Release kinetics of the paracetamol was observed to be very slow. The reason for this observation is attributed to hydrophobic interactions between the drug and the polymer/protein which accounts for a high loading efficiency and a non-efficient release kinetics.

Within the scope of the work, it is hereby claimed that the interactions between the drug and the nano-carrier plays a major role in determining both loading efficiencies and release kinetics. Further understanding of these systems require a complete matrix study of the various parameters responsible for altering these interactions – pH, temperature, nature of drug, surface functionalization of nano- carriers and so on.

Introduction

Nanoparticles (NPs) have undoubtedly become an important building block in many of today's industrial sectors. Core-Shell NPs in particular, have many potential applications in areas such as catalysis, biosensing and drug delivery.

Applications of NPs are based on the characteristic physical properties that stem from the small size of such particles, properties that differ from those in the bulk and molecular scale for the same material. One of the most interesting properties that stem from the small size of NPs, is a huge surface area that could be exploited for several applications like catalysis, bio sensing, theranostics and so on. Besides, these size-induced properties include, high reactivity, optical enhancement, mechanical, electronic and catalytic properties.

Ferromagnetic materials, such as iron oxides for example, when approaching the nano-scale they develop super-paramagnetism. This property develops because the particles become single domain magnetic materials with one high magnetic moment at room temperature.

Nobel metals such as silver and gold develop optical properties due to localized surface plasmon resonance (LPSR). The LSPR arises from the excitation of the electron cloud formed by the interaction of the large number of atoms that reside in the surface of the nanoparticles. Gold particles have shown also catalytic activity at the nano-scale and have been applied in reforming processes in the oil industry.

Nanoparticles synthesis can be classified in two categories, 1) the top-down approach and 2) bottom-up approach. Top-down approach consists mainly on mechanical reduction of the bulk material to the nano-scale. Using this approach gives very little control over particle size and shape, thus yielding a broad size distribution. Techniques such as attrition, milling and lithography are examples of this approach.

The bottom-up approach, on the other hand, consists on building chemically the nanoparticles up, from atoms and molecules. This approach requires a metallic salt precursor, a reducing agent and a stabilizing and/or capping agent. Nanoparticle synthesis through this approach is achieved by nucleation and growth of these particles in solution. Both nucleation and growth depend on the level of supersaturation in the solution, which is the driving force behind these processes.

Supersaturation can be defined in terms of the chemical potential 'μ' of the atoms or molecules in the solution, and in the bulk of the newly formed crystal phase as:

$$\Delta\mu = \mu_s - \mu_C$$

where μ_s and μ_c are the potentials in solution and crystal phase respectively. Supersaturation is achieved when $\Delta\mu > 0$ and only then is nucleation and growth possible.

Chemical potentials are defined in terms of standard potential μ_0 and activity a, by

$$\mu = \mu_0 + RT \log a$$

Substituting this equation and simplifying, the chemical potential can be express by:

$$\Delta\mu = kTln(S)$$

where k is the Boltzmann's constant, T is absolute temperature, and S is the supersaturation ratio, which is given by:

$$S = \frac{a_1^{n_1} a_2^{n_2} \dots a_j^{n_j}}{a_{1,e}^{n_1} a_{2,e}^{n_2} \dots a_{j,e}^{n_j}}$$

Here n_i is the number of the *i*th ion in a molecule of the crystal, a_i (m^{-3}) and $a_{i.e}$ (m^{-3}) are, the actual and equilibrium activities of the ions in the solution, and the denominator is the solubility product. Activities can be replaced by concentration terms in dilute solutions[29].

In supersaturated solutions the formation of a solid phase is energetically favorable; this solid phase implies the generation of an interface, which is energetically unfavorable. Hence for nucleation to occur, an energy barrier must be surpassed.

The overall excess free energy, ΔG, between a small nucleus of solute and the solute in solution is given by:

$$\Delta G = \Delta G_s + \Delta G_v$$

where $\Delta G_s$is surface excess free energy; the excess free energy between the surface of the particle and the bulk of the particle, and ΔG_v, is the volume excess free energy; the excess free energy between a large particle and the solute in solution. For a spherical particle

$$\Delta G = 4\pi r^2\gamma + \frac{4}{3}\pi r^3 \Delta G_v$$

Here γ is the interfacial tension between the growing crystalline surface and the supersaturated solution, and ΔG_v, is the free energy change of the transformation per unit of volume. The interfacial free energy is always a positive term and volume free energy is of opposite sign, and both terms depend differently on the radius. Therefore the free energy of formation goes across a maximum (ΔG_{crit}) at which the nucleus reaches an intermediate size as seen in the figure. Once the nucleus grows large enough otherwise know as the critical size r_c, the free energy of the system is decreased regardless of whether the nucleus grows or dissolves. At this point the rate of generation and growth of the new phase is then only limited by the rate of mass transport or energy[45].

Nucleation depends on the critical size r_c, and its relationship with the main external control parameter, the supersaturation, and the primary materials control parameter, the interfacial tension[45].

Nucleation can occur in the bulk solution, known as homogeneous nucleation, or it may occur on a surface readily available either from impurities or pre-synthesized nanoparticles, known as heterogeneous nucleation. The availability of the surface in heterogeneous nucleation changes the nucleation energy by a factor φ, dependent on the geometry of the surface, wetting and contact angles.

$$\Delta G_{heterogeneous} = \Delta G_{homogeneous} * \varphi$$

Therefore when $\varphi < 1$

$$\Delta G_{heterogeneous} < \Delta G_{homogeneous}$$

This is depicted in figure1. for a spherical particle, and this reduction in energy allows the formation of core/shell nanoparticles.

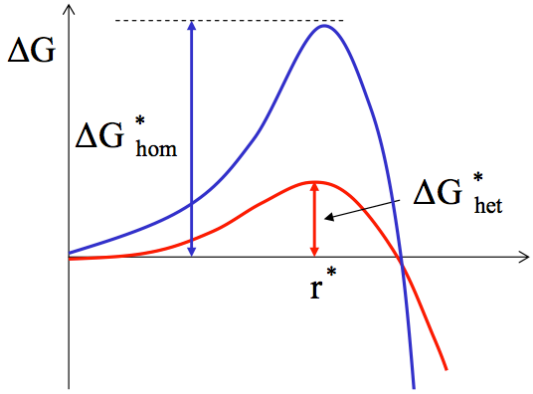

Figure 1. Gibbs free energy for homogenous and heterogeneous nucleation.

Above the critical energy both nucleation and growth occur simultaneously but

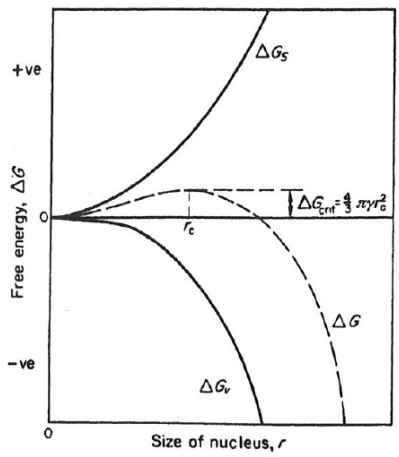

Figure 2. Graph Gibbs free energy as a function of nucleus size.

at different rates. Once the concentration of the solute decrease below the specific concentration for the critical energy nucleation stops, whereas growth of the nuclei will continue until the solubility equilibrium of the growing species is reached.

Two processes, diffusion and surface processes can control the subsequent growth of the nuclei. Diffusion controlled growth of the particle is controlled, as the name indicates, by the diffusion of the growing species from the bulk to the particle surface. This control occurs for example when the chemical reaction supplying the growing species is slow. Diffusion controlled growth promotes the formation of mono-dispersed particles.

If the diffusion of the growing species is fast enough, therefore making the concentration of the species at the surface of the particle the same as in the bulk, surface processes control the growth of the nuclei.

Surface processes follow two mechanisms: 1) mononuclear growth, where the growth proceeds layer by layer, since there is enough time for the diffusion of the growth species on to the surface of the growing particle; hence making the growth rate proportional to the surface area. 2) poly-nuclear growth, which occurs at very high surface concentrations. The growth of the second layer begins before the first layer is completed; therefore the growth rate is constant.

Core/Shell nanoparticles synthesis is two-step processes, involving first the synthesis of the core, followed by shell formation. Depending on the availability of the core particles the synthesis routes are classified in:

- Pre-synthesized core routes
- *In situ* synthesized core routes

For the pre-synthesized core routes, the core particles are synthesized separately, cleaned, dried and then added to separate reaction mixture for the shell synthesis. As for the *In situ* routes the core is synthesized, once formed, the reactants for the shell are added to mixture for shell formation.

Common methods for the nanoparticles synthesis include: chemical reduction in solvents, thermal decomposition, sol-gel methods, chemical vapor deposition, micro-emulsions, co-precipitation and hybrid methods.

Chemical reduction in solvents is the most common method for synthesis of metallic nanoparticles. This method consists in reducing the corresponding precursor by means of a reducing agent in solution, and requires the use of protective agents to avoid agglomeration and for the stabilization of the nanoparticles. The precursors may be elemental metals, inorganic salts, and metal complexes. Control over the shape and size of the nanoparticle can be achieved by adequate selection of the reducing agent

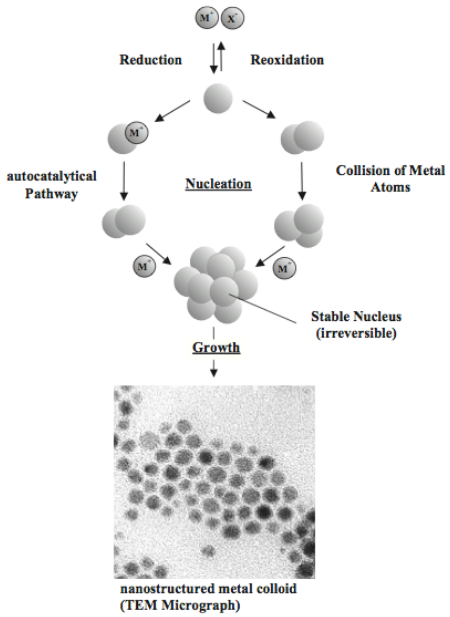

Figure 3 Chemical reduction of metallic presursor

and capping/stabilizing agent. Various reducing agents are available such as: sodium citrate, hydrogen peroxide, hydroxylamine hydrochloride, citric acid, carbon monoxide, phosphorus, hydrogen, sodium borohydride and hydrazine.

Sol- gel method is a wet chemistry process that combines a hydrolization step for a metal-alkoxide or metal precursor, leading to a solution of dispersed hydrated metal hydroxides followed by a poly-condensation step to form a three-dimensional network (gel). The gel is then dried, forming an ultra porous solid. [5]

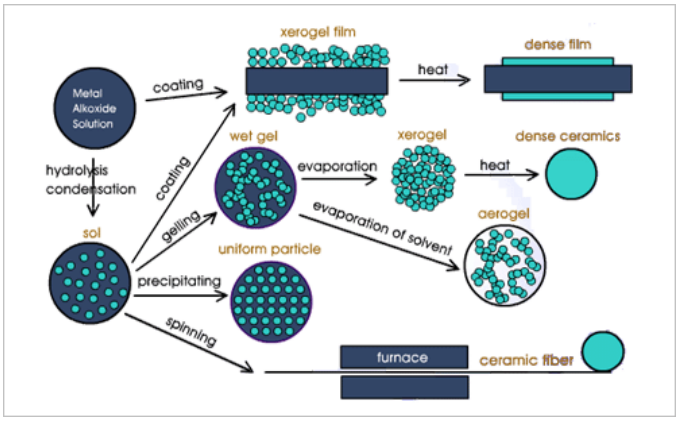

Figure 4 Schematic of sol-gel method

Particle size depends on the rate of hydrolysis and condensation, the solution composition, pH, and temperature [7]. Hydrolysis can be carried out either by a base or an acid.

Sol-gel synthesis can generate a variety of materials with different shapes, such as porous structures, thin fibers, nanoparticles and thin films.

For Thermal decomposition, organometallic compounds are decomposed to metals, by 1 of 2 methods; one method consists of introducing the reactants into a hot solvent containing a surfactant or alternatively, the reactants can be mixed at low temperatures and the resulting reaction mixture is gradually heated to generate the NPs.

This method provides precise control of the size and shape of the NPs through systematic modification of the reaction parameters, such as reaction time, reagent concentration (precursor, surfactant) and reaction temperature; the requirements for the latter range between 250 and 500º C [13].

After selective precipitation of the metal NPs, these must be washed several times with anhydrous alcohol to remove the surfactant to proceed with the shell synthesis.

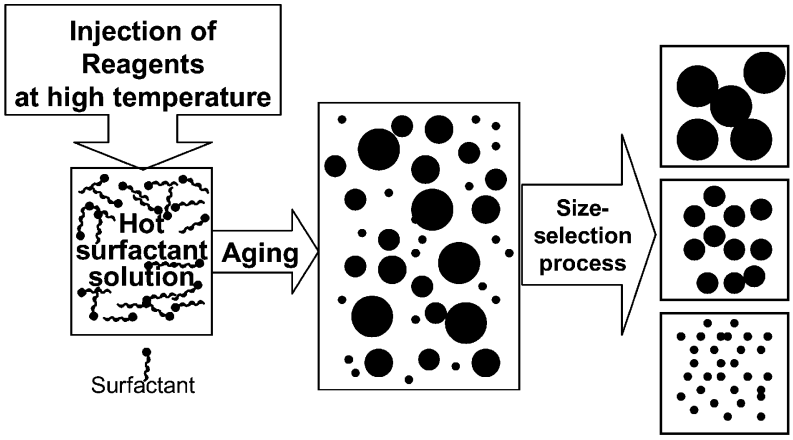

Figure 5 Schematic of thermal decomposition

Chemical vapor deposition is a technique in which the metal precursor is vaporized, then deposited on the wafer's (substrate) surface. Reaction occurs at temperatures over 900ºC in a heated reaction chamber[24].

At the vapor phase mixture, conditions of vapor supersaturation are reached in which it is thermodynamically favorable for the molecules to react chemically forming a condensed phase. If enough supersaturation is reached and depending on the reaction/condensation kinetics, homogenous nucleation will occur. [40]

Controlling the reactor temperature, precursor concentration or residence time allow control over the degree of supersaturation, which in turn controls the particle size. Rapid quenching of the system by rapid expansion of the two-phase gas stream leaving the reactor stops the reaction[40].

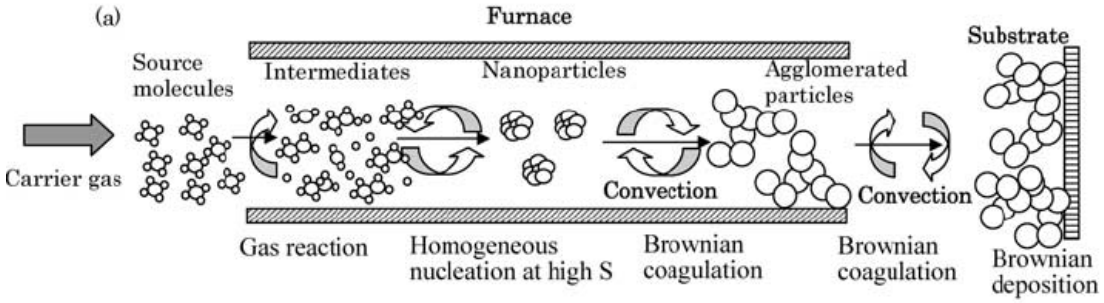

Figure 6 Illustration of vapour deposition technique

Micro-emulsion method consists in dissolving both the precursor and the reducing agent in two identical water-in-oil micro-emulsions. The aqueous phase containing

the precursor solution and reducing agent is dispersed within the reverse micelles, which are stabilized by an interfacial film of surfactant molecules. Then by mixing the two solutions, these micelles, subjected to Brownian motion, collide, coalesce and mix the precursor and reducing agent forming the nanoparticles, and then separating again into identical initial micelles.

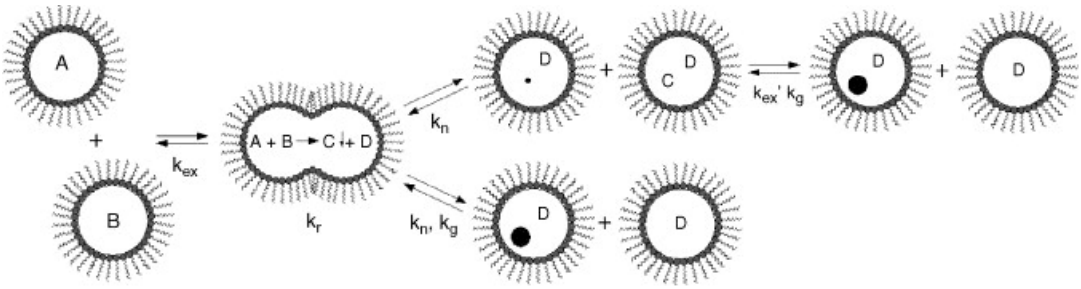

Figure 7. Mechanism of micelle based synthetic route

Since the micelles function as nanoreactors, controlling their size and shape also controls the size and shape of the nanoparticles. These are determined by the molar ratio of water to surfactant. The nanoparticles are then extracted by washing with solvents, such as acetone or ethanol, and redispersing in a given solvent.

Co-precipitation is another common straightforward method of synthesizing nanoparticles. The principle for this method is the precipitation of metal ions from aqueous salt solutions by addition of a base under an inert atmosphere either at ambient temperature or elevated temperatures. The shape, size and composition of the nanoparticles depends on the type of salts used, such as chlorides, sulfates and nitrates, the temperature of reaction, ionic strength of the solution and the pH value.

Drug Delivery

Drug delivery is the process of releasing a bioactive agent at a specific rate and at a specific site[39]. This process presents many challenges mainly because the majority of drugs are limited by characteristics as low solubility, high toxicity, non-specific delivery, degradation and short circulation lives[39]. The most challenging task in drug delivery is the passage of drug molecules across numerous physiological barriers[7, 11, 39].

Nanomaterials in Drug Delivery

Nanomaterials provide many great advantages for a broad range of applications. For drug delivery specifically, the small dimension of such materials provide properties, such as high surface to volume ratio which enables more drug to be attached on the surface; longer circulation times due to increased stearic hindrance and hydrophobic interactions, targeted drug delivery and reduction in toxicity. Nanomaterials can penetrate across barriers effectively through small capillaries, and hence providing efficient drug accumulation at the targeted site. Nanomaterials can protect drugs from degradation by harsh environments in the body, e.g. acidic pH in the stomach or liver enzymes[11], therefore increasing the drugs' bioavailability in the body. Nanomaterials have been applied in the treatment of cancer, infectious diseases, fungal and parasitic infections, bacterial infections, metabolic diseases and even viral infections[7].

Pharmacokinetics

Depending on the administration route of the drugs, these need to over come several barriers on its passage to the circulation system. Such barriers include: the stomachs acidic environment, proteases in the gut lumen and brush border membrane, tightly bound intestinal epithelial cells and enzymatic degradation.

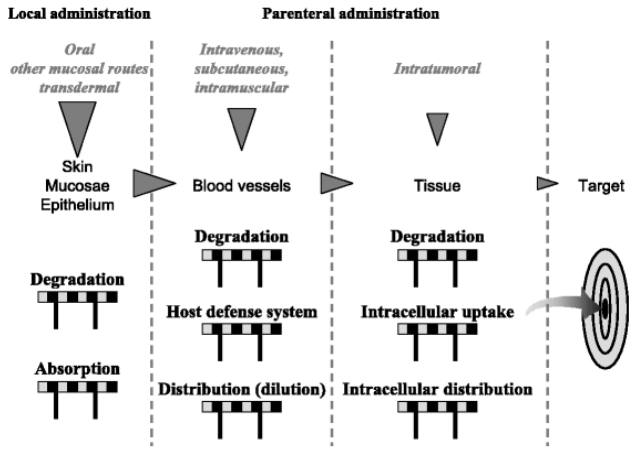

Figure 8. Drug admistration routes.

Drug administration routes can be classified in: local and parenteral routes[7]; local routes include oral, transdermal and other mucosal routes (pulmonary,

nasal, vaginal, rectal, etc.) and parenteral routes include intravenous, subcutaneous and intramuscular routes.

Intravenous administration has the advantage that the drug enters the bloodstream directly. Subcutaneous and intramuscular administrations provide a slow release of the drug into the bloodstream. Oral administration unlike other routes is considered the best route due to patient compliance although it is the route that has to overcome the most barriers in order for the drug to reach the bloodstream.

Once the drug has reached the bloodstream, distribution can take place. Distribution is affected by factors such as size, shape, surface charge and interactions with the immune system and serum proteins.

Drug metabolism is the enzymatic biotransformation of drugs[32]. The main organ that handles this process is the liver, although it is not the only one. Drug metabolism occurs once the drug exits the gastro intestinal tract, reaches the bloodstream and is carried to the liver. This metabolism by the liver enzymes is called the pre-systemic or "first-pass effect", and may result in partial or complete deactivation of the drug[32].

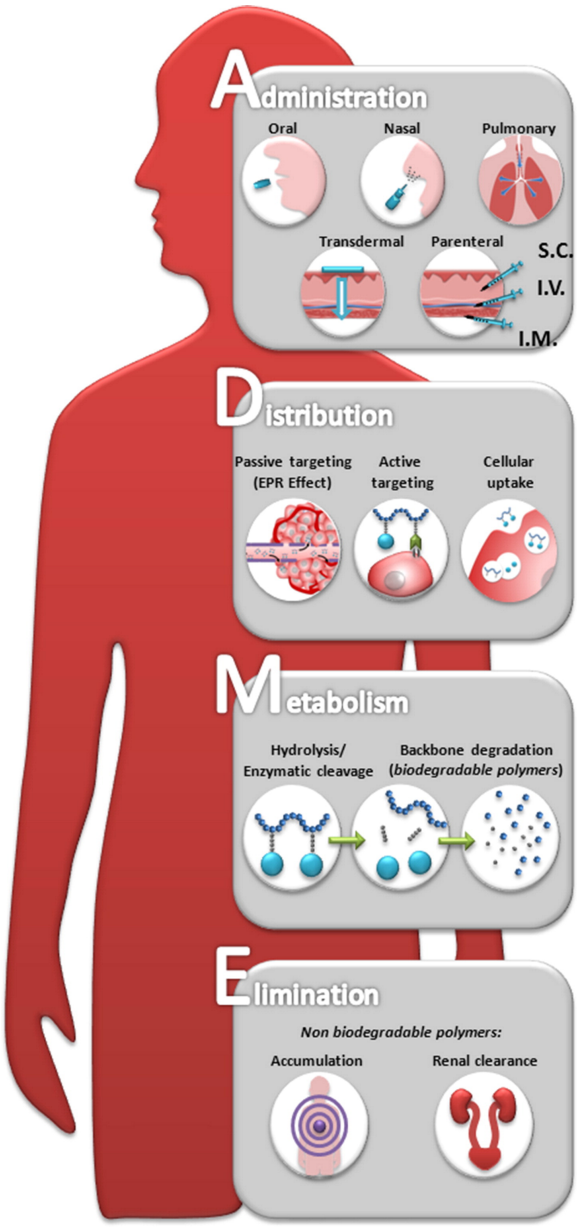

Figure 9. ADME diagram of drug pathway through the human body[11].

The first pass effect can be avoided by using alternate administration routes such as the intravenous route, but

eventually drugs in the bloodstream reach the liver. Further more other enzymes in tissues aside from the liver can also metabolize drugs.

Although the first pass effect is at first an undesired effect, once the drug has reached its target and carried out the desired effect, then, drug metabolism by the liver is desired, for this way drugs can be eliminated from the body.

Drug elimination is the removal of active drug from the body[31]. Drugs may be eliminated from the body in a chemically altered form or expelled in an unaltered form[14]. There are three principle routes for drug elimination; in bile through the liver (hepatic elimination), in urine through the kidneys (renal elimination) and in exhaled air through the lungs (pulmonary elimination)[14, 31].

In hepatic elimination, enzymes in liver reduce, oxidize, hydrolyze or form conjugates drugs, with the purpose of converting drugs into water-soluble compounds for easy excretion through the bile. The bile then enters the digestive system where lipid soluble drugs may be reabsorbed and the rest eliminated through faeces.

Renal elimination is only possible if the drug or conjugate are water-soluble and if their molecular sizes are not to big. Strong adsorption to proteins in the bloodstream also interferes with this elimination process. Renal elimination is carried out mainly by membrane filtration and transport against a chemical gradient[14, 31].

Pulmonary elimination is the route that contributes the least to drug elimination. It is the main route for elimination of volatile drugs, and most are eliminated in an unaltered form since these compounds suffer little or no metabolism in the body. [14, 31]

Therapeutic index, loading efficiency and encapsulation capacity

The use of nanoparticles for drug delivery can reduce the dose-limiting effects of highly toxic drugs, by means of targeted drug delivery. Targeted delivery implies

obtaining high concentrations of the drug at the desired site while at the same time minimizing its presence at other sites.

Targeted delivery can therefore improve drug properties such as the therapeutic index (TI). TI is the ratio between the maximum tolerated toxic dose and the minimum effective dose, represented by:

$$TI = \frac{MTTD}{MED}$$

The higher the values of TI the safer the drug is.

Toxicity of the drugs refers to the presence of the drug at the toxic sites where unwanted side effects are expressed. Loading of drugs onto nano-carriers can therefore reduce the concentration of drug at toxic sites, elevating the values of MTTD and hence increase the TI values of toxic drugs[39]. The amount of drug that can be loaded onto a nanocarriers is known as the loading efficiency. It is calculated by:

$$L.E. = \frac{C_i - C_f}{C_i}$$

Where C_i is the initial drug concentration in the solution and C_f is the free drug concentration after a loading in a certain period of time[26, 47].

It is needless to say that high loading efficiency is desired for effective drug delivery; nonetheless, obtaining high values of L.E. is limited by the accessibility of binding sites and drug diffusion to the surface of the nanoparticle, depending on the loading pathway[10]. During drug loading the properties of both, the nanoparticle and the surrounding environment, depend on the nanoparticle design, such as core material and coating ligand for the former and medium properties, such as ionic strength and type of solvent for the latter.

An important parameter for nanoparticle delivery systems is the Encapsulation capacity (EC) of the nanoparticles. This defines the drug carrying capacity of such systems. EC of the nanoparticles is calculated according to the following equation[26, 47]:

$$EC = \frac{C_i - C_f}{C_n}$$

where C_i and C_f are the total initial and the final free concentrations of the drug, and C_n is the nanoparticle concentration.

EC of nanoparticles is dependent on the interactions between the drug and the nanoparticle. These interactions themselves are dependent also on the nanoparticle design and surrounding environment, as for the loading efficiency.

Drug Delivery Modes

Previously drug delivery systems have been developed for conventional routes of drug administration, such as oral and intravenous. Even though in actuality alternate routes of administration or so-called non-conventional methods are being thoroughly investigated, drug delivery modes can be classified in two categories: conventional and controlled.

Conventional drug delivery consists of periodic administration of the drug, resulting in a constant change in the systemic drug concentration with periods of ineffectiveness and toxicity[35]. Conventional drug delivery, can therefore, also be classified as uncontrolled drug delivery since, there is no control over the therapeutic concentration of the drug in the body.

Controlled drug release, as the name states, maintains the therapeutic drug concentration in body for an extended period of time. This is achieved by controlling the rate of delivery of the drug. Today, various rate-controlling mechanisms are available, such as matrix diffusion, membrane diffusion, and biodegradation, to mention a few[35].

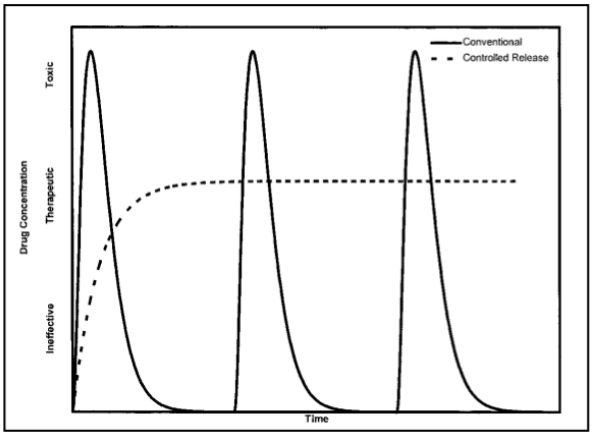

Figure 10. Diagram illustrating controlled and conventional drug release.

Another objective of drug delivery systems is drug targeting. Drug targeting is essentially the high efficient pathway between drug-release from a specific point to a pre-determined site, obtaining high local concentrations of the drug at the desired site.

Commonly, drug targeting is dependent of free transport; this is the convection of free drug in the bloodstream with possible circulation towards the diseased tissue[16]. This dependence is due to the fact that the target of all administration routes is delivering drugs to the bloodstream. Once in the bloodstream, drug targeting can be achieved by either of two methods, passive targeting or active targeting.

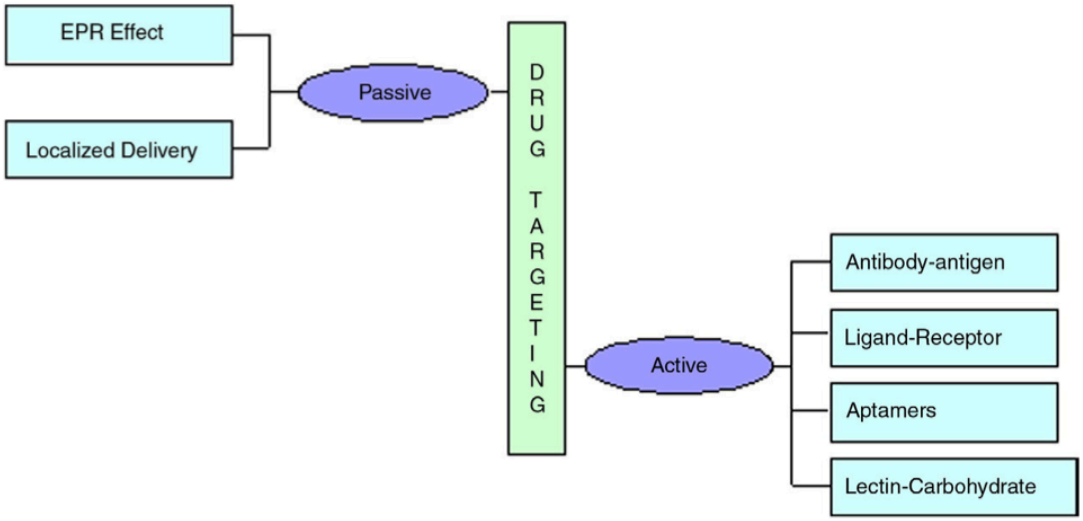

Figure 1. Diagram illsutrating modes of passive and active targeting[39].

Passive Targeting

Passive targeting refers to non-specific accumulation of macromolecules or nanoparticles on inflammatory, infectious or tumor sites. It is dependent on the anatomical differences between diseased and normal tissues. Diseased tissues develop a defective vascular architecture, giving way to hyper-permeability of the blood vessels and thus allowing the accumulation of macromolecules or nanoparticles in the matrix of such tissues. This is known as the Enhanced Permeability and Retention (EPR) Effect[10, 16, 39].

In some cases, diseased tissues, such as tumors, can develop an impaired lymphatic drainage system leading to ineffective liquid removal[39], and hence increasing the EPR effect. The EPR effect is depicted in the diagram in figure…

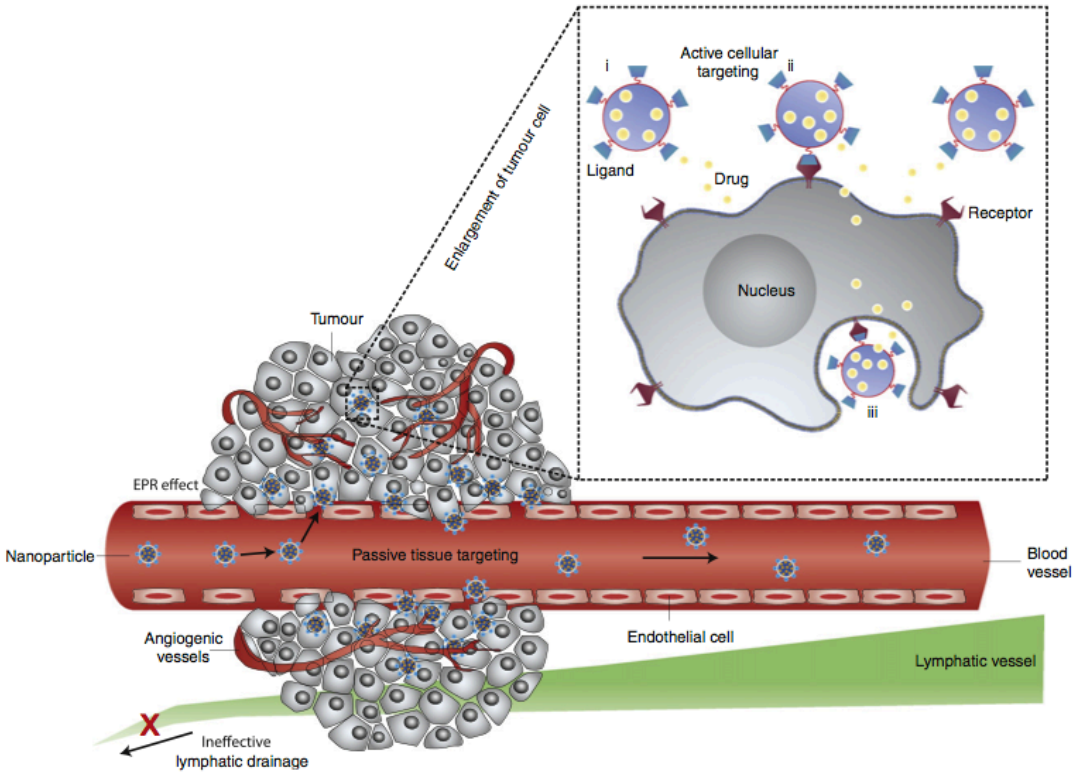

Figure 11. Diagram of passive targeting in conjugation with active targeting[10].

Another way of passive targeting is localized delivery[39]. This route is mainly applicable for tumors, since it implies direct intratumor delivery of the macromolecules or nanoparticles.

Active Targeting

In Active targeting, local concentration of the drug at the targeted site is increased through receptor specific ligands attached to the drugs' surface, which bind to receptors expressed at the targeted site[8, 16, 39]. Therefore the effectiveness of active targeting depends greatly upon the selection of an adequate targeting ligand. Hence the targeting ligand should be abundant, have high affinity and specifity for binding to the receptor, and well suited to chemical modification by conjugation[39]. On the other hand, the targeted receptor should be expressed homogeneously over the cells in the targeted tissues.

Targeting ligands can be antibodies, aptamers (DNA or RNA oligonucleotide sequences) peptides, vitamins or carbohydrates[16]. Active targeting is often coupled with the EPR effect as seen in the diagram.

Functionalization of core-shell NPs

Core-shell NPs prove of great advantage in drug delivery[4, 10], it can be inferred that the core-shell design is the most important and widely applicable model when it comes to any field of biotechnology and biomedical science[4]; none the less they are rarely used as prepared substances because they need to fulfill certain criteria in order to be used in biomedical applications[41]. These criteria include minimal cytotoxicity, avoidance of non-specific interactions with plasma proteins, depending on their application; allow or avoid uptake by the reticuloendothelial (RES) system and maintain colloidal stability under physiological conditions[41]. In order to comply with such criteria NPs need to be functionalized.

Functionalization can be either achieved during the synthesis of the particles (*in situ* functionalization) or after synthesis of the NPs (post functionalization). The former case is preferred when one-pot synthesis methods are aimed at. This could be due to competitive binding of adsorbents onto the NP surface, which may be favored under certain synthetic conditions, whereby subsequent addition of surface modifiers can be carried out. On the other hand, post

functionalization may be desired when polarity of the NPs change dramatically after functionalization – Fe NPs synthesized in an organic phase cannot be functionalized in an organic environment, because the aim might be to use them for biological applications, where water solubility becomes an important issue.

Functionalization is achieved through surface modification; this is introduction of a chemical functional group on the surface of the nanoparticles. This can be achieved by conjugation of other functional ligands, by electrostatic interactions, hydrophobic/hydrophilic interactions, covalent bonding and so on.

A simple method for surface functionalization is the layer-by-layer self-assembly. As the name suggests, it implies the formation of consecutive surface monolayers. The driving force behind the multilayer build up include interactions such as: electrostatic and donor/acceptor interactions, hydrogen bonding, adsorption/drying cycles, covalent bonds and stereocomplex formation or recognition[23]. *Lee et al* have successfully accomplished layer-by-layer assembly through electrostatic interactions for Au NPs for target specific intracellular delivery[20].

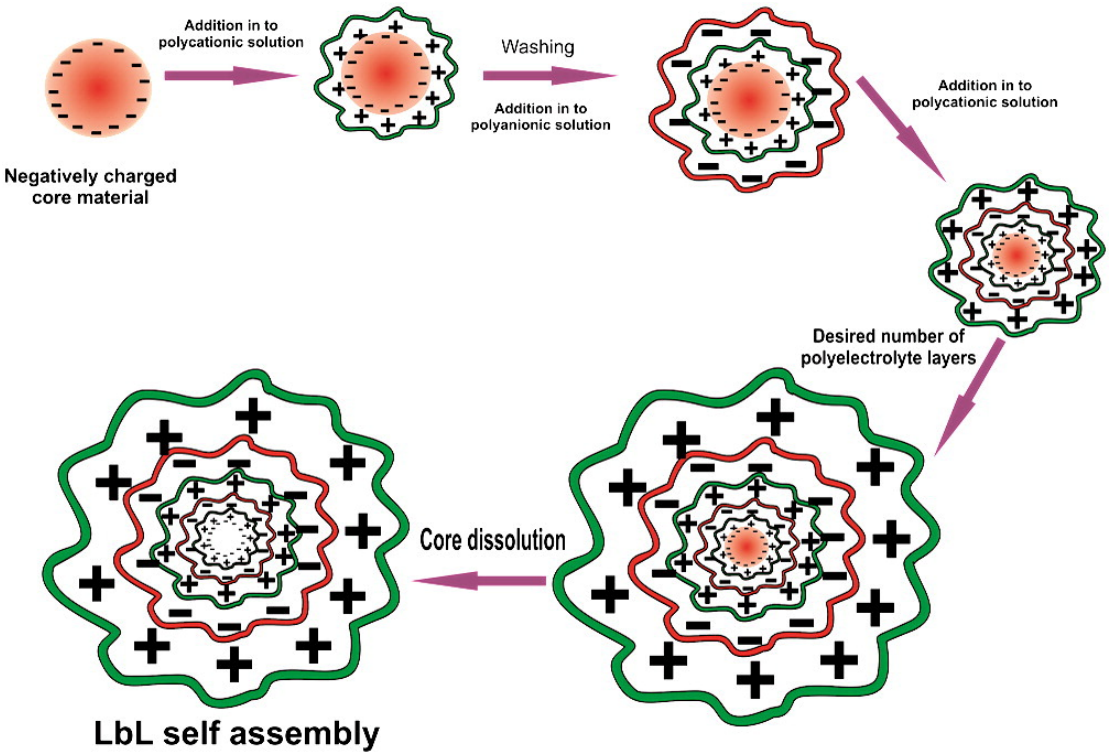

Figure 12. Diagram depicting Layer-by-Layer self-assembly[9].

Electrostatic interactions driven Layer-by-layer self-assembly, results from the alternation of surface charge for each consecutive layer, giving great freedom in the number of layers as well as the layering sequence[9]. A more thorough review on layer-by-layer self assembly was performed by *Deshmukh et al*[9].

The advantages of this technique are that it is not specific to electrostatic forces, requires no complicated equipment, and layer thickness can be controlled. A variety of chemical moieties such as, polymers, proteins, polynucleic acids, viruses, polymetallic clusters, etc., can be used to form the multicomponent particle.[23]

Coating with functional molecules

Due to precipitation induced by physiological salt concentrations ionically stabilized nanoparticles are generally unsuitable for biomedical application[38, 41]. Additionally once in the bloodstream, NPs are easily absorbed by plasma proteins in the RES system reducing their half-life. Coating with functional molecules provides NPs with colloidal stability in biological media, reduce cytotoxicity and specific targeting.

Coating of NPs surfaces can be done with: polymers, either natural or synthetic, small-molecule ligands, carboxylic acids, proteins, peptides, phospholipids, carbohydrates.

The use of polymers in drug delivery has gained much interest recently, since they show promising potential for tissue targeting, higher circulation times, convey protection against drug degradation, reduce drug toxicity,[30] and allow controlled drug release through degradable linkers[6]. All these properties stem from the multiple functional groups, such as carboxylic acids, phosphates, hydroxyls and sulphates that such molecules may contain.

In addition to the afore mentioned properties, polymers can respond to external stimuli, somewhat resembling the behavior of biological systems in a crude way[30]. Within the common stimuli, temperature, pH, ionic strength, light and redox potential are considered the most important[30]. The use of stimuli responsive polymers can be seen through out a great number of applications[30]. Temperature and pH-responsive polymers are of great interest in drug delivery, since drug release can be triggered by these stimuli which can be found in the human body environment; like the body's response in increased temperature related to infection and inflammation processes, and variation of pH within different tissues and cellular compartments[30].

Thermo-responsive polymers

The main characteristic of temperature responsive polymers is a sharp change upon a modest change in temperature. In case of biomedical application, the concerning change is a volume phase transition between hydrophobic and hydrophilic states in their structure, making the chains collapse or extend in aqueous media[30]. The temperature at which this transition occurs is known as the critical solution temperature (CST)[1]. Polymers, which become insoluble upon heating have a lower critical solution temperature (LCST), while on the other hand polymers that become soluble upon heating have an upper critical solution temperature (UCST)[30].

Polymers with LCST aggregate at temperatures above the LCST, therefore enabling thermal drug targeting. In this sense the thermo-responsive polymer being soluble in biological media, would become insoluble and accumulate at heated site[6]. To accomplish this the transition temperature should greater than the physiological body temperature (37ºC) and lower than the temperature of the heated site[6].

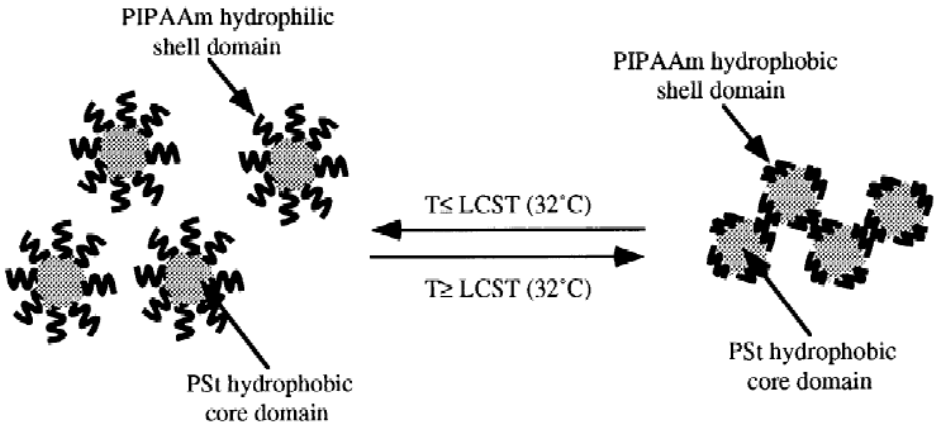

Figure 13. Diagram depicting collapse of thermo-responsive polymer at LCST[3].

The most studied thermo- responsive polymer is Poly(N-Isopropylacrylamide) (PNIPAM), due to the closeness of its LCST (approx. 32ºC) to that of the human body temperature. Further more, the LCST of PNIPAM can be modified by copolymerization or conjugation with others hydrophilic polymers.[5, 6, 30] However, the use of PNIPAM is limited in *in vivo* applications due to its non biodegradability and the presence of amide moieties which reduce the polymers biocompatibility[12]. *S.Cammas et al* have used PNIPAM as site-specific drug carrier[3].

pH-responsive polymers

pH-sensitive polymers are polyelectrolytes that contain within their structure weak acidic or basic groups able to accept or release protons as a response to a change in the pH of their surroundings[28]. As thermo-responsive polymers, pH-responsive polymers suffer conformational change resulting in swelling or dissolution, with the difference that this change is driven by ionization and the

factors controlling this change are now the pH and ionic composition of the aqueous medium. [28]

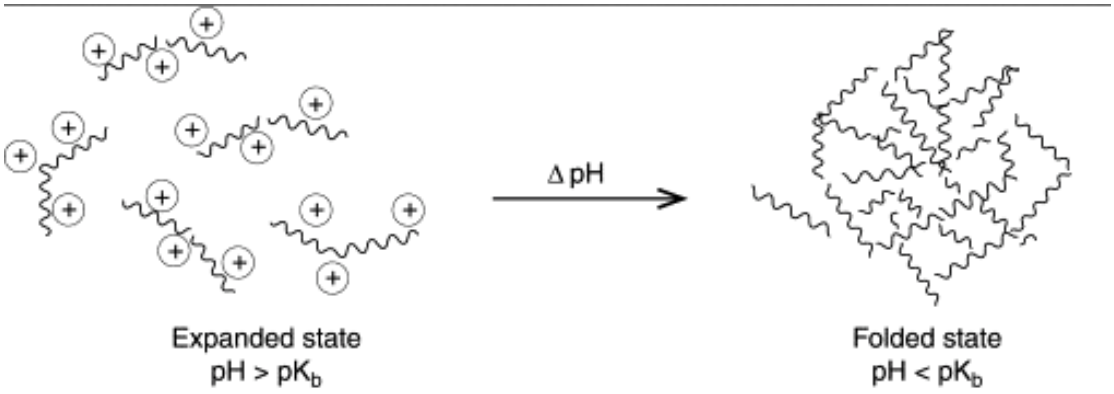

Figure 14. Diagram depicting the confortmational change of pH-responsive polymers.[28]

The conformational change that pH-sensitive polymers under go are due to two electrostatic interactions; interactions between polymer chains and interactions between polymer chains and water molecules. The pH-induced change will depend on the nature of the polyelectrolyte, whether if it is anionic or cationic.

In case of the anionic polyelectrolytes, polyacidic polymers will contract at low pH, while polybasic polymers will dissolve or swell at high pH. The complete opposite behavior is seen in case of cationic polyelectrolytes; polyacidic polymers will swell or dissolve at low pH and polybasic electrolytes will contract at high pH values.[28]

Proteins

Proteins are polymeric compounds of amino acids, linked to linear sequences by amide bonds[34]. They are commonly formed by a sequence of 20 different amino acids linked together, which provide them with different side chain residues. Proteins posses one carboxylic acid and one primary amino terminal group, in addition to the other functional groups or properties introduced by the amino acid side chains, which are dependent on their molecular structure. Properties such as charge, polarity and hydrophobicity are dependent of the amino acid sequence.

Proteins have secondary and tertiary structures as a result of folding which are determined by the afore mentioned properties. The inside of the protein is normally hydrophobic whilst the exterior is hydrophilic as a result of the amino acid side chains directed outward toward solution. The folding conformations of the proteins are stabilized by disulphide bonds forming between cysteine residues.

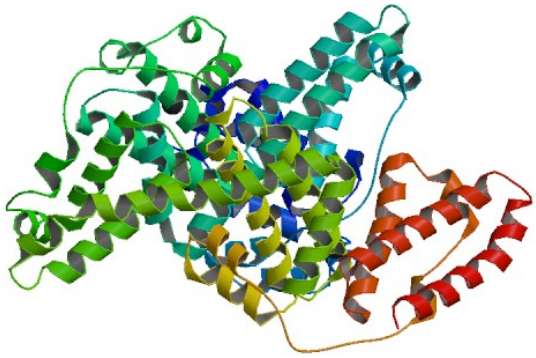

Figure 15.Illustration of folding conformation of protein molecules.

Conjugation with proteins allow NPs to interact with biological systems while at the same time providing NPs with functionality such as specific binding by molecular recognition other wise known as targeting. The conjugation of proteins with NPs is possible through: electrostatic interaction, Van der Waals forces, hydrogen bridges, thiol bonds or hydrophobic interactions[34].

Drug Loading

Drug loading can be carried out during particle formation/functionalization (*in situ*) or after particle formation/functionalization (*ex situ*)[15, 18, 42]. All drug-loading schemes are based on covalent or non-covalent approaches, where covalent methods involve chemically bonded linkers and non-covalent methods involve all other means of drug loading including hydrophobic, electrostatic, hydrogen bonding, and stearic immobilization[10]. Further more these approaches can be classified in encapsulation, surface mediated, and entrapment techniques[39].

Factors influencing the extent of drug loading are method of preparation, additives (stabilizers), nature of drug and drug carrier (chemical structure, hydrophobicity), solubility and pH[15].

Methods for drug loading include:

- Incorporation; incorporation of the drug into the polymer matrix during particle formation during mixing[25] (crosslinking of polymers).
- Incubation; adsorption to the surface or entrapment of the drug from solution[33]. Incubation time and drug-carrier interactions influence greatly the efficiency of this method. Incubation time has to be enough to reach equilibrium for maximum drug loading and the drug needs to interact preferentially with the carrier[15].

Drug Release

In drug delivery the drug release from the NPs is equally or more important than drug loading for the development of an effective delivery system. Usually a sustained constant concentration of the active compound in the blood is desired, though it is not the only drug release profile desired[1]. Literature describes 5 different highly desired release profiles.

1. Conventional delay but not constant release.
2. Constant or zero-order release
3. Substantial delay followed by constant release
4. Delay followed by tight pulse release
5. Multiple pulses at specified periods.

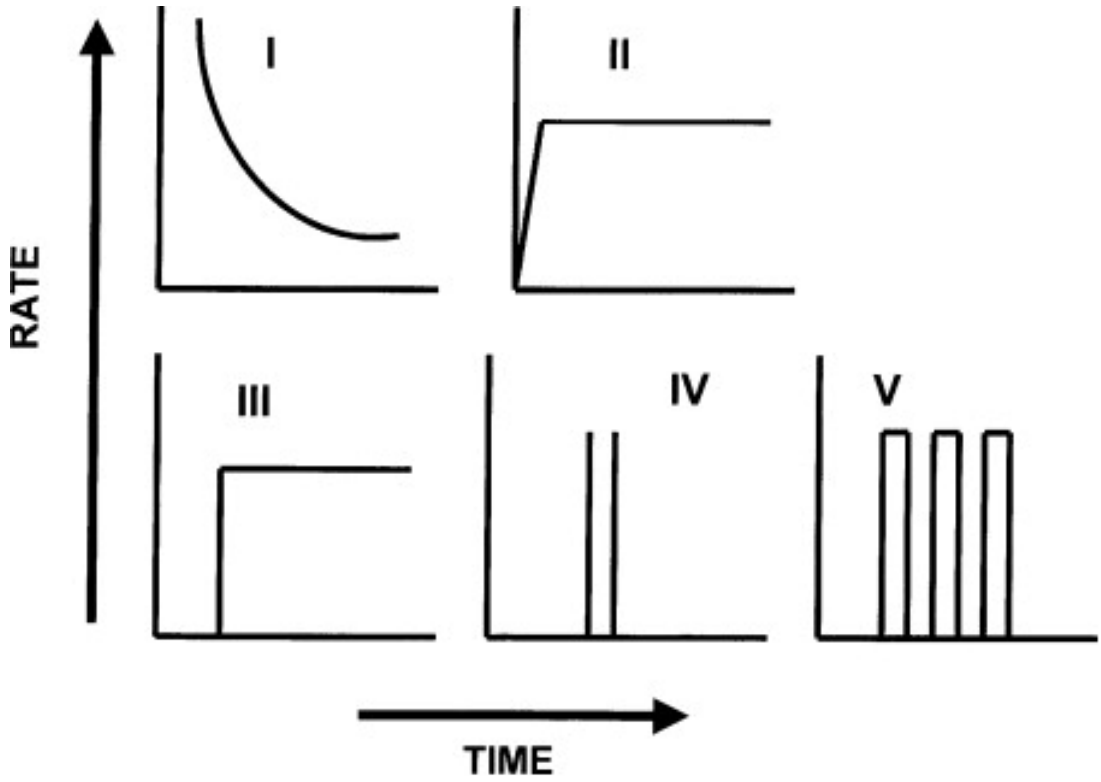

Figure 16. Diagrams of drug releasing profiles.[1]

Drug release occurs through a series of mechanisms, which are dependent on the way the drug incorporation route; drugs bound/adsorbed to surfaces desorb, diffusion through the nanoparticle matrix, diffusion through the polymer wall of nanocapsules, nanoparticle matrix erosion or a combined erosion-diffusion process. In essence drug release is governed by diffusion and biodegradation[33].

Diffusion drug release mechanism

Diffusion drug release mechanism is derived from Fick's second law of diffusion and is described by the following equation[44]:

$$\frac{M_t}{M_o} = 4\left(\frac{Dt}{\pi h^2}\right)^{\frac{1}{2}}$$

where M_t, is the amount of drug released at time t, M_0 is the total mass of drug loaded to the device, D is the diffusion coefficient of the drug with the carrier and h is the thickness of the device. For this mechanism there is no degradation or mass loss of the bulk material.

Degradation drug release mechanism

For this mechanism, drug molecules are chemically bonded to the polymer backbone therefor drug release is onset by hydrolytic or enzymatic cleavage. The rate of drug release is hence determined by the rate of hydrolysis[1].

Materials and Methods

Materials

Deionized water with a resistivity of at least 18.0 MΩ was used in all experiments. PNIPAM, amine terminated, poly-L-Lysine (PLL), sodium borohydride (Sigma-Aldrich), iron (II) chloride (Fisher), sodium citrate (Fisher), silver nitrate (Sigma-Aldrich), bovine serum albumin (Sigma-Aldrich), were used as purchased. N-acetyl-p-aminophenol (paracetamol) obtained from Jens Peters Lab, and BSA gold nanoclusters had been previously synthesized in the lab.

Synthesis of Fe@Ag NPs

Fe@Ag NPs where synthesized by reduction in homogenous solution at ambient conditions, modifying the procedure described by Carroll et al. Briefly, Fe@Ag NPs where prepared by mixing 1.25 ml of 4.6mM $FeCl_2$ solution and 1.25 ml of 0.46mM sodium citrate ($Na_3C_6H_5O_7 \cdot 2H_2O$) solution for 10 minutes with magnetic stirrer. Then 2.5 ml of 8.8mM NaBH4 solution prepared in-situ, no more than 2 minutes before addition and ice cold, were added drop wise under vigorous stirring and left to react for 5 minutes. This was followed by the addition of 2.5 ml of 2,5mM $AgNO_3$ solution drop wise, under vigorous stirring and left to react for 10 minutes. The reaction was quenched adding 7.5 ml of ethanol, centrifuged and redispersed in 10ml of mQ water.

Coating of Fe@Ag NPs

Coating of Fe@Ag NPs was carried out by incubation of the NPs in the respective polymer solution. 5 ml of the NPs solution where centrifuged for 15 minutes at 14500g. The supernatant of the solution was carefully discarded and the

precipitated particles where then redispersed in equal volume of the polymer solution under sonication. Once the particles where completely dispersed the solution was kept under constant shaking for 3 hours. After incubation particles where centrifuged to remove free polymer, redispersed in mQ-water and characterized with UV-Vis, DLS and ζ-Potential.

Drug Loading

PNIPAM and Poly-L-Lysine coated particles. Drug loading was done by incubation of the pre-coated particles in drug solution. The concentration range of the drug solution was 1, 2.5 and 5 mg/ml of Paracetamol. Particles where first, separated by centrifugation for 15 minutes at 14,500g. Supernatant was then removed and the precipitated particles where redispersed in the drug solution under sonication. Once dispersed the particle-drug solution was shaken for a minimum of 18 hours.

BSA coated particles. Two protocols where used: 1) Coating with paracetamol loaded BSA; BSA (0.7 mg/ml) molecules where dissolved in drug solution (1, 2.5 and 5mg/ml) and shaken for a minimum of 18 hours. Then Fe@Ag NPs solution was centrifuged for 15 minutes at 14,500g, supernatant discarded and precipitated particles were redispersed in BSA/paracetamol solution under sonication. After redispersion, the solution was shaken for minimum of 18 hours. 2) Incubation of BSA coated particles in drug solution; NPs where centrifuged for 15 minutes, supernatant was removed and precipitated particles where redispersed in drug solution (1, 2.5 and 5 mg/ml) under sonication. Once dispersed the particle-drug solution was shaken for a minimum of 18 hours.

Modified BSA. Freeze-dried BSA gold nanoclusters where redispersed in the paracetamol solution (1,2.5 and 5 mg/ml) and shaken for a minimum of 18 hours.

Release

Drug release was carried out in water and phosphate buffer saline solution, at 37ºC under magnetic stirring for 24 hours. The total sample was divided into 3 equal aliquots; at fixed time intervals (1, 3 and 24 hours) the concentration was measured.

Characterization Techniques

Scanning (Transmission) Electron Microscopy [S(T)EM]. S(T)EM images were acquired using a Hitachi S-5500 electron microscope operating at 30kV accelerating voltage. TEM images were obtained in bright field mode. TEM grids were prepared by placing several drops of the solution on a Formvar carbon coated copper grid (Electron Microscopy Sciences) and wiping immediately with Kimberly-Clark kimwipes to prevent further aggregation owing to evaporation at room temperature.

Dynamic Light Scattering [DLS]. The size distribution and zeta potential of the NPs were measured using a Malvern Zetasizer Nano-ZS instrument, and the manufacturer's own software. The solvent used for the NPs was mQ water.

Ultraviolet-Visible Spectroscopy [UV-Vis]

UV-Vis spectra were acquired with a UV-2401PC (Shimadzu) spectrophotometer. The spectra were collected over the spectral range from 200-800 nm.

X-ray Photoelectron Spectroscopy (XPS). XPS analyses were performed using a Kratos Axis Ultra DLD spectrometer (Kratos Analytical, UK), equipped with a monochromatized aluminum X-ray source (Al, hυ = 1486.6 eV) operating at 10 mA and 15 kV (150 W). A hybrid lens (electrostatic and magnetic) mode was employed along with an analysis area of approximately 300 μm X 700 μm. Survey spectra were collected over the range of 0-1100 eV binding energy with analyzer pass energy of 160 eV. XPS data were processed with Casa XPS software (Casa Software Ltd., UK).

Results and Discussion

Physicochemical Characterization of Fe@Ag NPs

Fe@Ag NPs were synthesized using a solution based synthetic route, employing sodium borohydride as the reducing agent and Na-citrate serves the purpose of both a passivating ligand and a partial reducing agent. The Fe precursor is initially reduced by the strong reducing agent, $NaBH_4$ to form small Fe NPs. These Fe NPs serve as nucleation centres for the formation of the Fe@Ag NPs. The heterogeneous nucleation initiates with the addition of the Ag precursor (generation of chemical supersaturation). As the supersaturation is slowly consumed through the formation of the core shell structures, growth of these particles continue mainly through agglomeration of pre-formed particles, until the reaction is quenched using ethanol. This bottom-up approach of synthesis ensures a homogeneous particle distribution with an easily tunable citrate coated surface. The surface modification with citrate enables a wide range of functionalization options besides allowing for stability in the aqueous medium.

The size of Fe@Ag NPs was determined by dynamic light scattering (DLS) and transmission electron microscopy (TEM).

TEM imaging (Fig 17 (a),(b)) show that the particles are spherical, which is advantageous since high curvature is needed to minimize clearance by macrophages and the ideal size of nanocarrier should be between 10 and 100 nm[8, 25]. The difference in size using different characterization techniques can be attributed either due to DLS measuring the hydrodynamic rather than the core radius of the NPs as measured by S(T)EM, a weak interparticle dipolar interaction among NPs causing weak interparticle coupling, or a combination.

XPS survey spectrum (Fig 17(c)) confirms that there are compositionally two different phase materials in the nanoparticles, Fe and Ag. In the survey spectrum, the XPS peak for Fe 2p can be observed around 707eV while the peak for Ag 3d can be seen around 369 eV which matches with previously reported XPS data for similar NPs.[46]

UV-Vis absorption spectra (Fig 17(c)) of the Fe@Ag NPs, shows an LSPR spectra at 406 nm, characteristic of Ag NPs, therefore confirming the optical signature of these constructs.

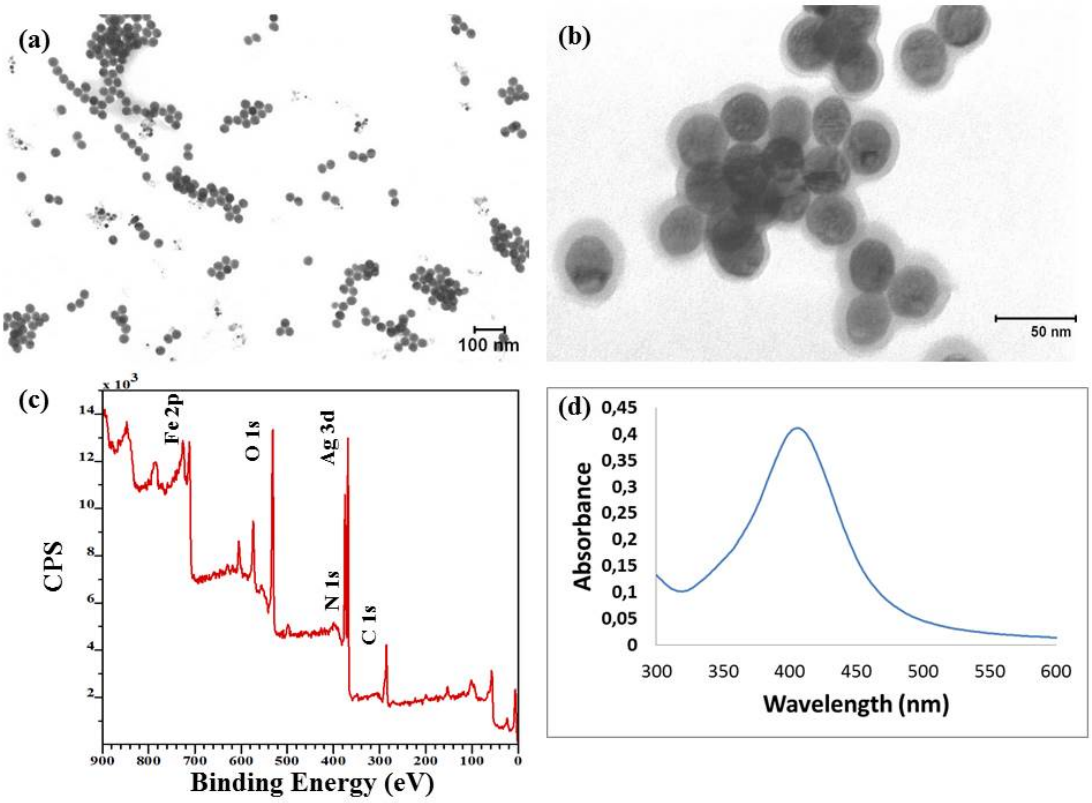

Figure 17. (a) and (b) respresentative S(T)EM images ,(c) XPS Survey Spectra and (d) UV-Vis absorbtion spectra of Fe@Ag NPs.

These new particles show a ζ-potential of – 25.7 ± 0.6 mV. This high value accounts for the electrosteric stability of the particles in aqueous solution, possibly enabling prolonged circulation times for *in vivo* applications.

Paracetamol is a standard drug used for experimental studies at the lab scale. It is p-aminophenol derivative and is the most common used analgesic and antipyretic (fever reducing) agent. It is completely adsorbed from the intestinal tract and metabolized by the liver. At high concentrations it can cause hepatic injury.

Paracetamol Calibration Curve

Paracetamol is a standard drug used for experimental studies at the lab scale. It is p-aminophenol derivative and is the most common used analgesic and antipyretic (fever reducing) agent. It is completely adsorbed from the intestinal tract and metabolized by the liver. At high concentrations it can cause hepatic injury,

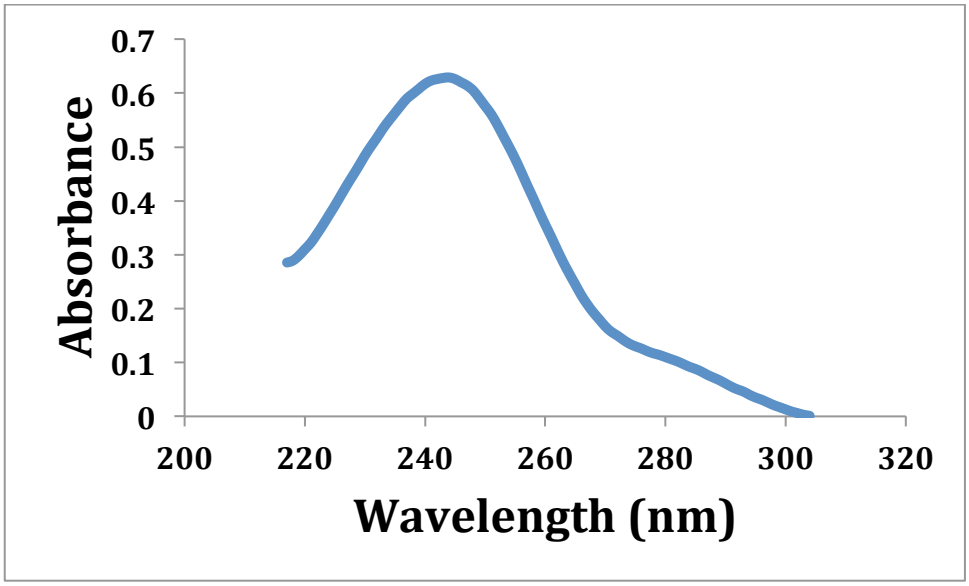

Figure 18. UV-Vis spectrum for paracetamol.

A standard calibration curve for paracetamol (Fig 19) was generated by measuring the absorbance values at 243nm (the wavelength, at which maximum absorbance is reported for the drug) for different known concentrations of the drug. The calibration curve is valid for concentrations ranging from 0.001 to 0.025 mg/ml within which the absorbance values follow Beer - Lambert's law. A linear regression equation is fitted to the data to yield a linear function between absorbance and concentration of paracetamol. In subsequent measurements care has been taken to carry out necessary dilutions to have the measurable concentrations within the range.

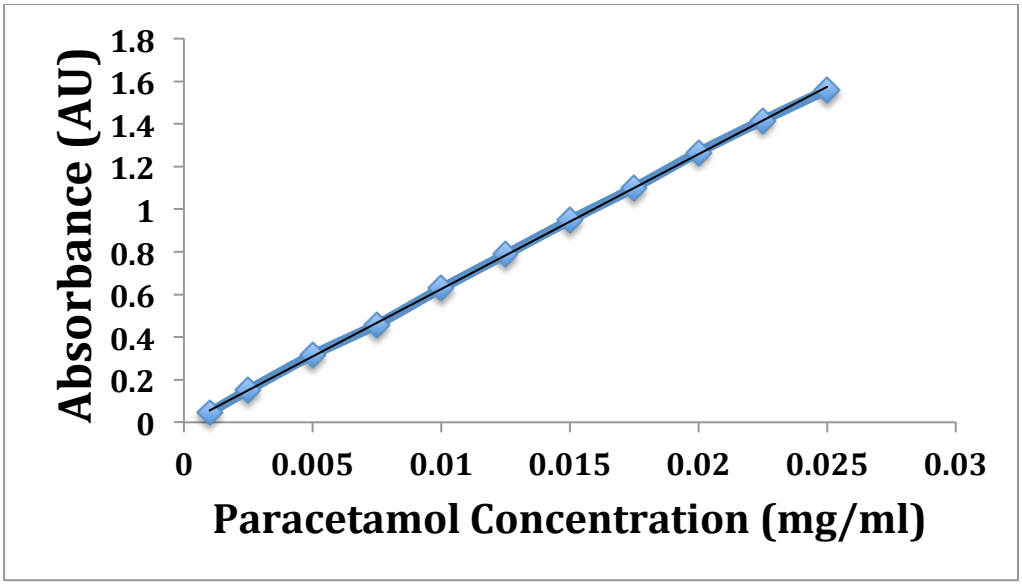

Figure 19. Paracetamol calibration curve.

The regression equation obtained is $A = 63.286c - 0.0077$ with a correlation coefficient of 0.9998, where A is the absorbance and c the concentration (mg/ml) of drug in aqueos phase.

Physicochemical Characterization of Functionalized Fe@Ag NPs

The zeta potential of the Fe@Ag NPs (Fig 20)increase upon functionalization with PNIPAM and PLL functionalization. These indicate coating of the NP surfaces with the respective polymers. However, Fig 21 suggests that there is also increase in size upon polymer coating. This is attributed to loose aggregation among the functionalized particles owing to the presence of charged polymers.

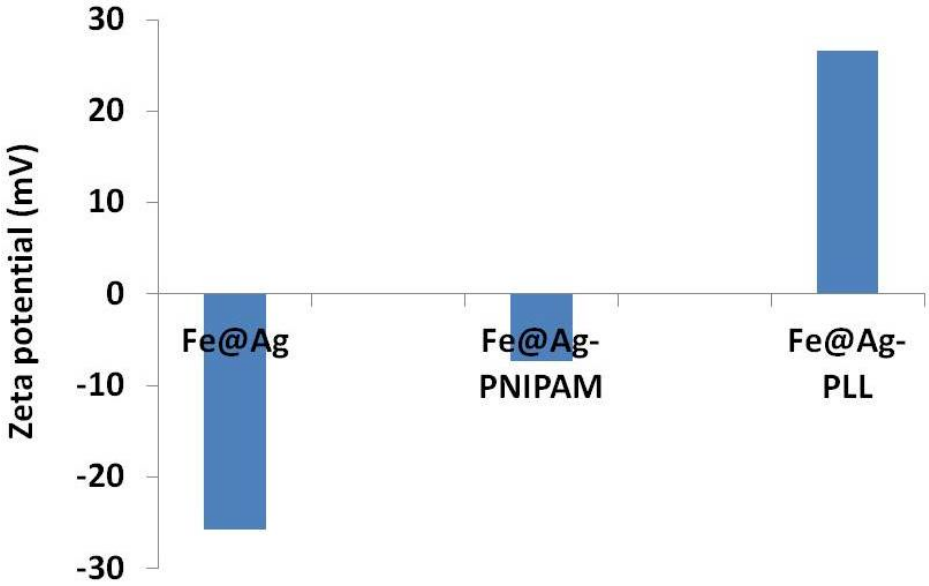

Figure20. Zeta potentials of bare Fe@Ag NPs and polymer coated Fe@Ag NPs.

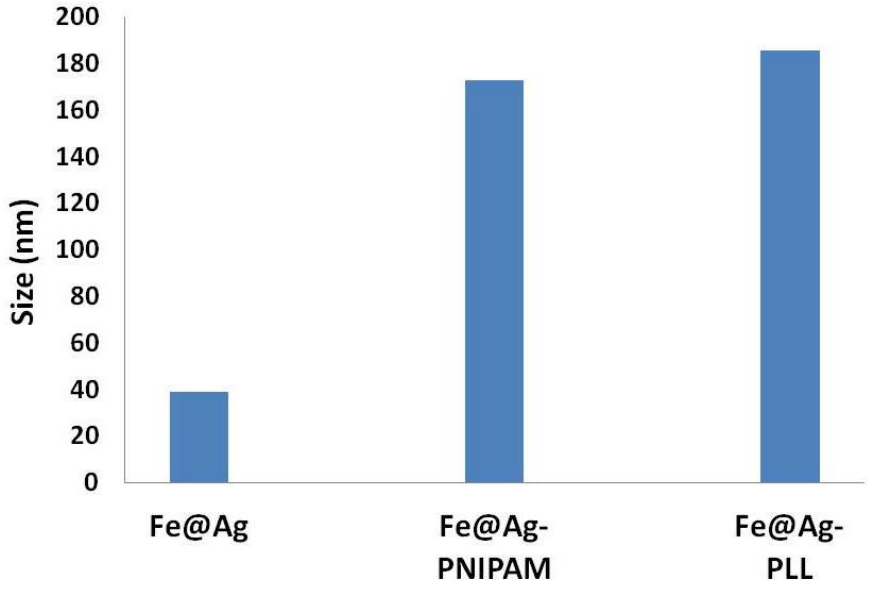

Figure 21. DLS sizes of bare Fe@Ag NPs and polymer coated Fe@Ag NPs

Loading Efficiency

The drug carrying capacity of a nanoparticle delivery system is defined as a loading efficiency. Paracetamol loading was carried out by the incubation method, for a minimum of 18 hours to ensure the onset of equilibrium to achieve maximum drug loading.

Effect of PNIPAM and Poly-L-Lysine

Loading of paracetamol was done on two different batches of Fe@Ag NPs one functionalized with PNIPAM and the other with Poly-L-Lysine (PLL).

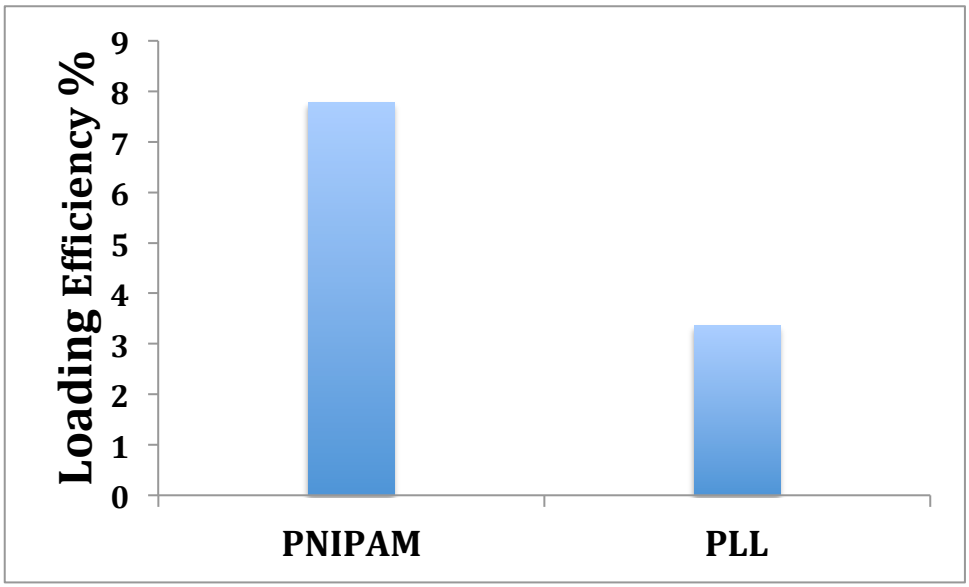

Figure 22. Loading efficiencies for Fe@Ag NPs coated with PNIPAM and PLL for 5 mg/ml of paracetamol.

Loading efficiencies obtained for NPs coated with PNIPAM (7.78%) and PLL (3.35%) are shown in figure 22. Results show that the PNIPAM coated NPs present higher loading. Although this is not in line with the studies done by *Villiers et al.*[15], which state that drug loading can be improved by increasing polymer concentrations or employing polymers with higher molecular weights; this can be attributed to the fact that Paracetamol has a lower electrostatic repulsion toward PNIPAM than PLL. From Fig 23, the molecular structure of both polymers and paracetamol, it can be observed that PNIPAM (m.w. 4500) has *n+1* number of electron pairs from the nitrogen groups, where n is the degree of polymerization. In the case of PLL (m.w.150.000), there are *2n* number of electron pairs, where n is comparatively higher than that for PNIPAM, giving the latter a more dense electronic cloud. Interactions between the drug molecule and the polymer are assumed to be comprising mainly of electronic cloud overlap, which should show an opposite trend. However, electron density matching is expected to be better for the paracetamol- PNIPAM interaction, owing to secondary amine repeat structures (increased electronic cloud over nitrogen owing to positive inductive effect from the attached methyl groups) as compared

to primary amine repeat units in case of PLL. It is also hypothesized that the interactions between the paracetamol and polymer are mostly hydrophobic. This leads to the fact that the relative position of the drug in these nanoconstructs might be a guide to the loading efficiencies. PLL, having a higher molecular weight, would hinder diffusion of the small paracetamol towards the NP surface (more than PNIPAM), whereby yielding a higher loading for the PNIPAM coated NPs.

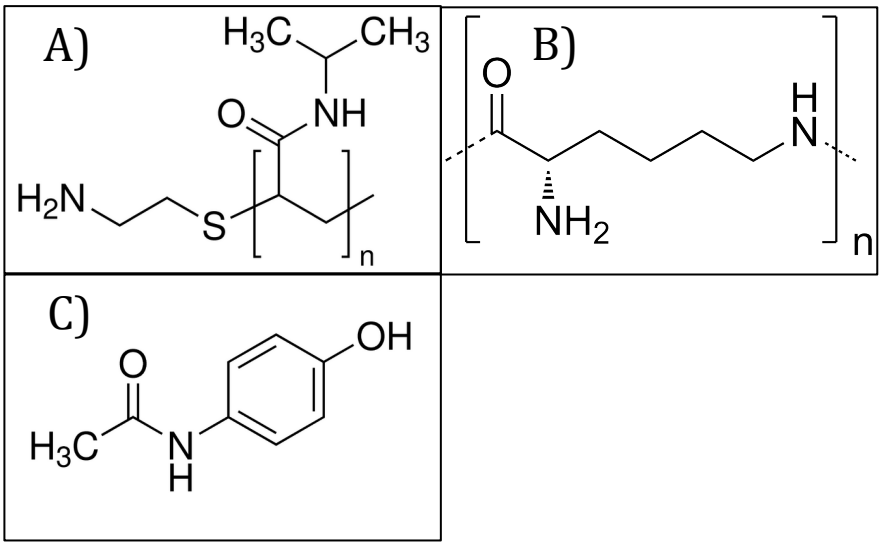

Figure 23.Molecular Structure of (A) Poly(N-isopropylacrylamide), amine terminated (B) Poly-L-Lysyine and (C) Paracetamol

Even though drug loading was obtained with PNIPAM and PLL, further studies were not continued with these constructs as these loading efficiencies were considered to be on a lower side. Further, drug delivery applications require introduction of nanocarriers that are either already in use or are of very low toxicity when introduced in the body. In this regard, BSA was chosen to be the desired nanocarrier as it has already been used as a carrier for many drugs including paracetamol. Although BSA has been widely studied in terms of its interaction with Au NPs[2], there has not been enough research on using these conjugated BSA NPs for efficient drug delivery.

Effect of BSA

Albumin is the most abundant serum protein responsible for transport of both, compounds that originate in the body and compounds alien to the body[37]. In

addition BSA is a biopolymer carrier that is being evaluated as a drug delivery system in the treatment of cancer[17].

For *Protocol 1* in BSA experiments, a maximum of 8.3% loading efficiency was obtained with 5mg/ml concentrations of paracetamol, using 0.7 mg/ml of BSA protein for coating and functionalization of the Fe@Ag NPs.

In this study, Paracetamol loading efficiency was affected by the initial concentration of paracetamol in the loading media, as seen in Fig 24, higher loading efficiencies where obtained for higher initial concentrations. This tendency was observed despite the use of different loading protocols Fig….

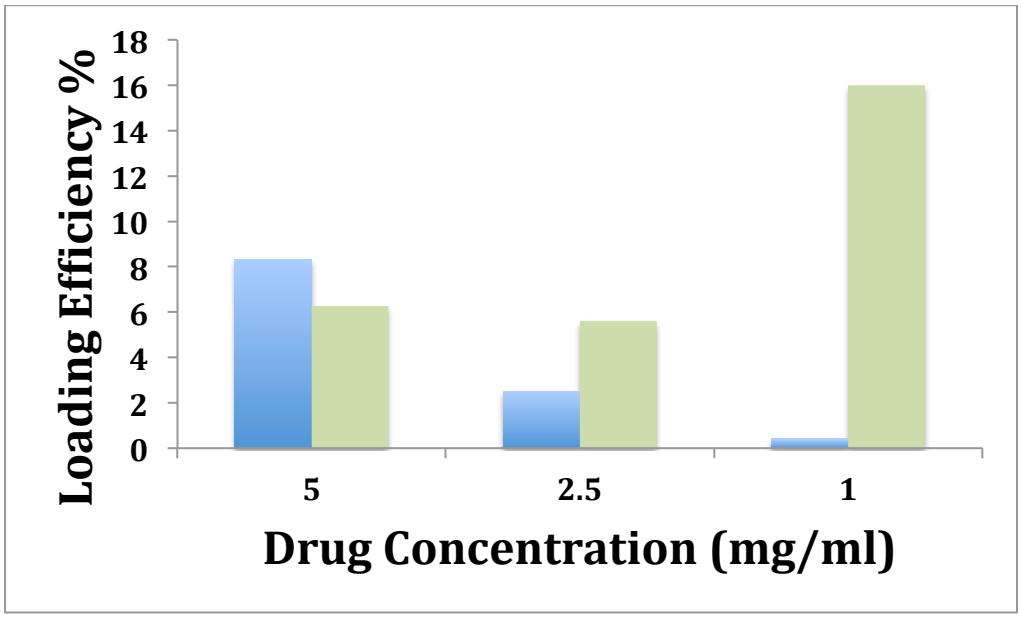

Figure 24. Loading Efficiency as a fucntion of paracetamol concetration. (blue) Protocol 1 and (green) protocol 2.

However a loading maximum was observed at 5 mg/ml of paracetamol after carrying out drug loading experiments with an initial paracetamol concentration of 10mg/ml and obtaining a lower loading efficiency (4.58%) than with 5 mg/ml concentration (8.32%). Assuming that the maximum loading capacity (MLC) of BSA has been reached in both scenarios, this shows that the loading efficiency is also dependent on the particle concentration. The entrapment efficiency does not necessarily increase with higher initial drug loading. According to *Gaber et al*[15] once the MLC of the carrier is reached, further increase in the initial drug

concentration can decrease the efficiency. Thus, it is felt worthy to study the complete matrix by varying particle concentration, BSA concentration and drug concentration to conclude on the mutual influences of the parameters.

The higher drug loading can be attributed to the higher concentration gradient of the paracetamol in solution, which is known to be the driving force for the diffusion and adsorption processes.

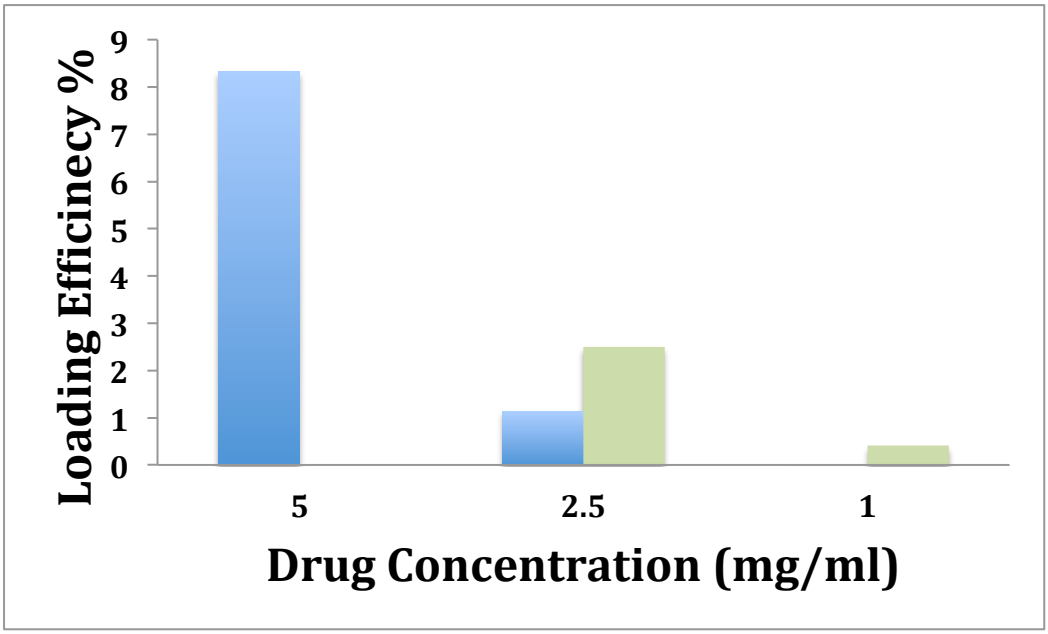

Figure 25. Loading efficiency as a fucntion of paracetamol concetration. (green) Loading efficiencies with dilution factor corrections.

The measurement of paracetamol concentration was done using UV-Vis spectrometry; the absorption values must lie between 0 and 1 in order to comply with the linearity of *Beer-Lamberts* law; operating principle of the equipment. Therefore the solutions had to be diluted to a concentration of 0.01 mg/ml of paracetamol in order to obtain appreciable absorption values. Lower concentration values increase the error in concentration measurement, as can be seen in Fig 25. For the 2.5 and 1 mg/ml concentration assays the samples where diluted 500 times resulting in 0.005 mg/ml and 0.002 mg/ml of paracetamol respectively, even though this values lie within the calibration curve, appreciable errors of 55% and 100% respectively can be observed in the calculated concentration from these measurements and those done when the same samples where diluted 250 and 100 times respectively to obtain the desired 0.01 mg/ml

concentration of paracetamol. It is also important to note that at these measurement concentrations, no LSPR peak is observed for the particles. Further support to no obvious interactions between the drug and the NPs during the UV-vis studies is guaranteed by no appreciable shift of the paracetamol absorbance peak, upon adsorption to the NPs. This also points to the fact that free paracetamol concentration is being measured in all these experiments.

During *protocol 2,* adsorption of paracetamol onto BSA-coated NPS, the interaction between BSA and paracetamol discussed could not be quantitatively used to determine the loading of the drug into BSA. This is because; it was impossible to separate the free paracetamol from the BSA and loaded paracetamol through centrifugation. However, when UV-Vis was used to analyze the sample (BSA and paracetamol) at the start and end of loading, a significant drop in absorbance was noted (Fig 26). Although, this refers to the total decrease in the free paracetamol, it is difficult to ascertain this decrease to a decrease in the free paracetamol or bound paracetamol without performing separation. However, it may be mentioned that there is no significant change in UV-Vis peak position for the paracetamol.

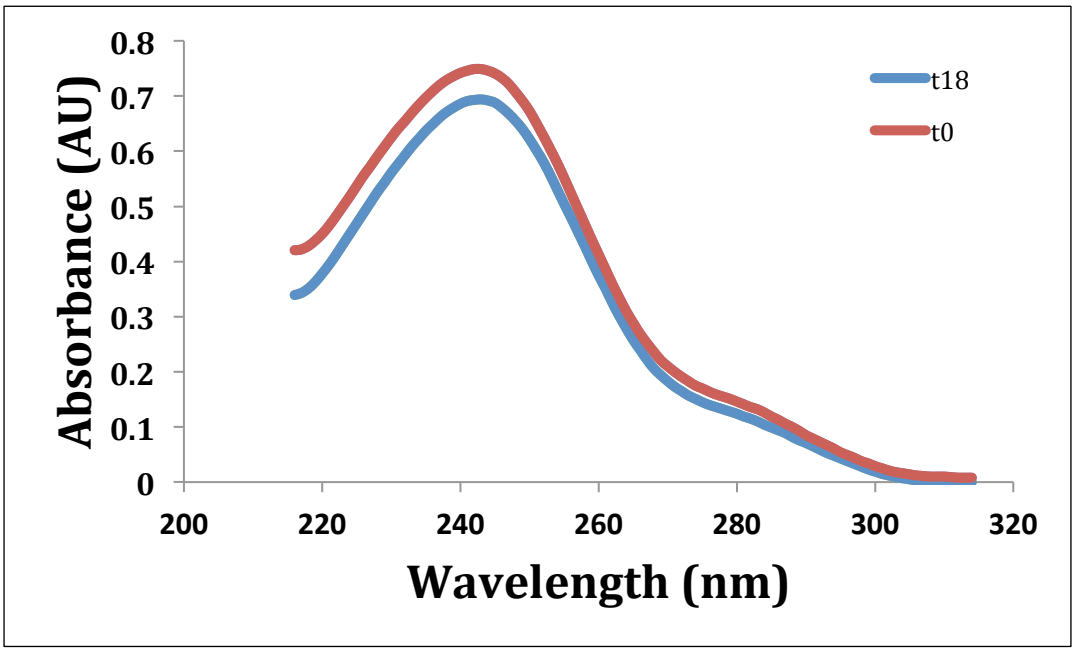

Figure 26. UV-Vis absorbance spectrum of paracetamol-BSA solution before and after incubation.

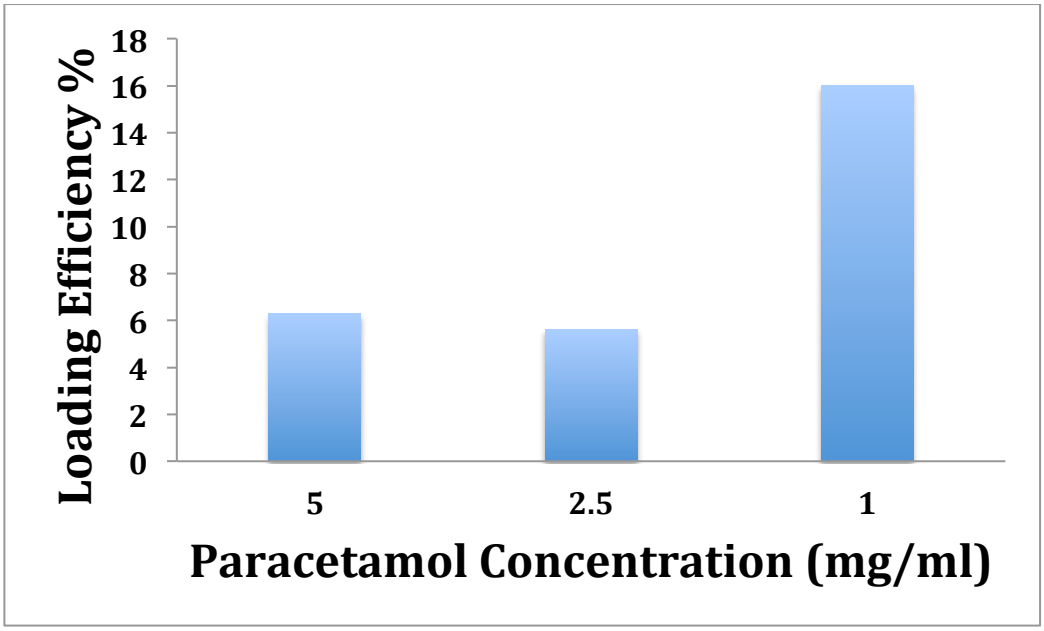

Figure 27. Loading efficiency as a function of paracetamol concentration. Loading following protocol 2.

For *protocol 2* in BSA experiments, a maximum loading efficiency of 16% was obtained with 1mg/ml concentrations of paracetamol, using 0.7 mg/ml of BSA protein for coating and functionalization of the Fe@Ag NPs. This result while it is the most promising result obtained during the course of the project; needs to be further investigated. Nonetheless it gives way to consider the influence of the conformational differences of BSA at the moment of drug loading, it's interaction with paracetamol and the Fe@Ag NPs.

BSA-Fe@Ag and BSA- paracetamol interactions

The nature of the interaction between BSA and Fe@Ag NPs is considered to be electrostatic. This can be concluded due to the fact that the isoelectric point of BSA is between 4.5 and 4.9[27], and experiments where carried out with mQ-water which has a pH of 5.6 above the proteins isoelectric point. A Zeta-potential value of -20mV for the Fe@Ag-BSA NPs, further more confirms this which is in accordance to studies performed by *Ravidran et al*[27]. The way BSA attaches to the NPs though is not known, and two mechanisms are suggested: either "brush conformation" or wrapped conformation"[27], in which case the brush conformation attachment is considered to yield higher loading efficiency; this considering the higher ratio of BSA molecules to NP under this conformation. In

addition binding of paracetamol occurs on two sites according to *Sułkowski et al*[37]. Hence, a higher ratio of BSA molecules to NP yields more paracetamol loading.

Although the highest drug loading efficiency obtained (16%) in this research, which was carried out following *protocol 2* for BSA with 1 mg/ml of paracetamol, does not follow any of the observable trends, it can be explained also in terms of conformational changes. Though in this case, these conformational changes are within the protein structure, for BSA shows great conformational adaptability[22]. *Sułkowski et al*[37] suggests there is a third binding site for paracetamol on BSA, which might not be exposed due to the folding conformation of the protein. Adsorption of BSA onto the silver coated particles might induce a conformational change in the BSA structure[21], making this third site exposed and thus allowing a third paracetamol molecule to adsorb. It can be further hypothesized that this conformational change, through stearic effects affects the attachment modality of the BSA molecule itself from the wrapped conformation to the brush conformation. A higher loading efficiency obtained (5.61%) using 2.5mg/ml paracetamol with *protocol 2* than with *protocol 1* gives further reason to this notion but it is difficult to clarify this without further investigation.

Effect of Particle concentration

Literature states that the high surface area of nanoparticles is one of their properties leading to higher drug loading[43]. Therefore nanoparticle concentration and hence surface area was investigated. As concluded from figure 27 higher loading was achieved for higher particle concentration. For low concentrations (1mg/ml) of nanoparticles no loading was observed, this can be attributed to the insufficient surface area for the BSA binding.

To corroborate that higher particle concentrations yielded higher L.E., different particle concentrations from the same batch of nanoparticles where tested under the same drug concentration (5 mg/ml). From figure 28 we can confirm that higher particle concentrations, and therefore increased surface area in fact yield higher loading efficiencies.

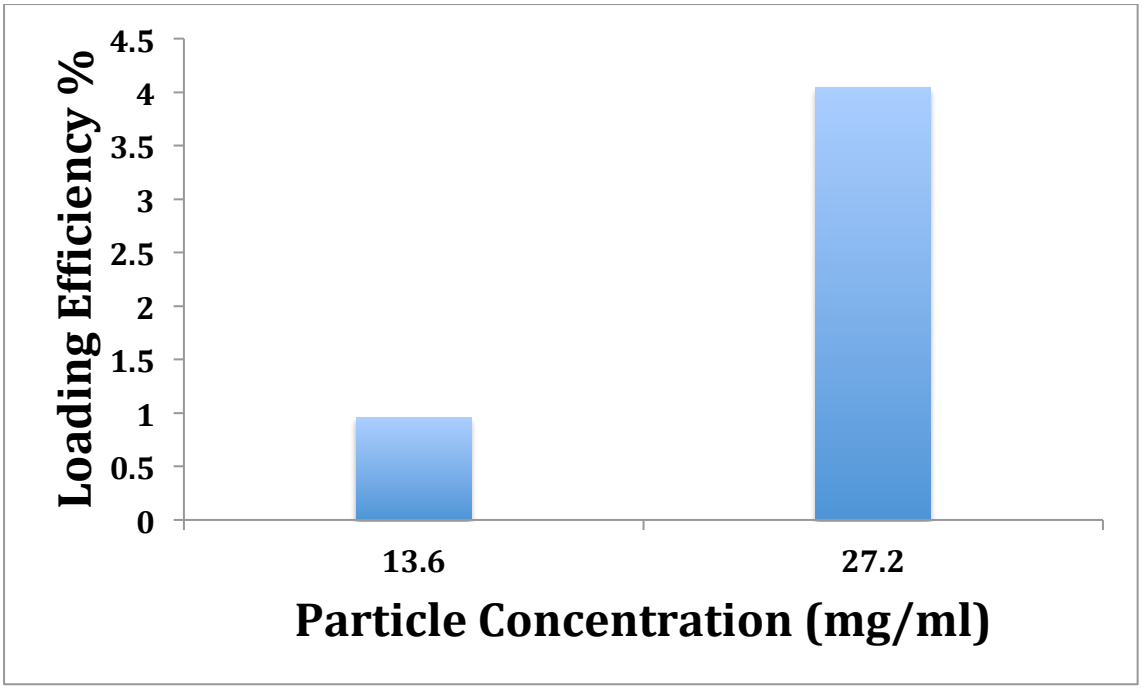

Figure 28. Loading efficiency as a fucntion of particle concetration for 5 mg/ml paracetamol concentration.

Loading Efficiency Modified BSA Nanoconstructs

On the notion of perturbed protein conformation trials using modified BSA protein with gold nanoclusters as the core-shell nanocarrier were carried out. Drug loading was observed in these new nanoconstructs at lower particle concentration; 1 mg/ml of BSA and 5 mg/ml of paracetamol yielded a maximum L.E. of 6%. Lower paracetamol concentration yield lower L.E. as seen in fig 29.

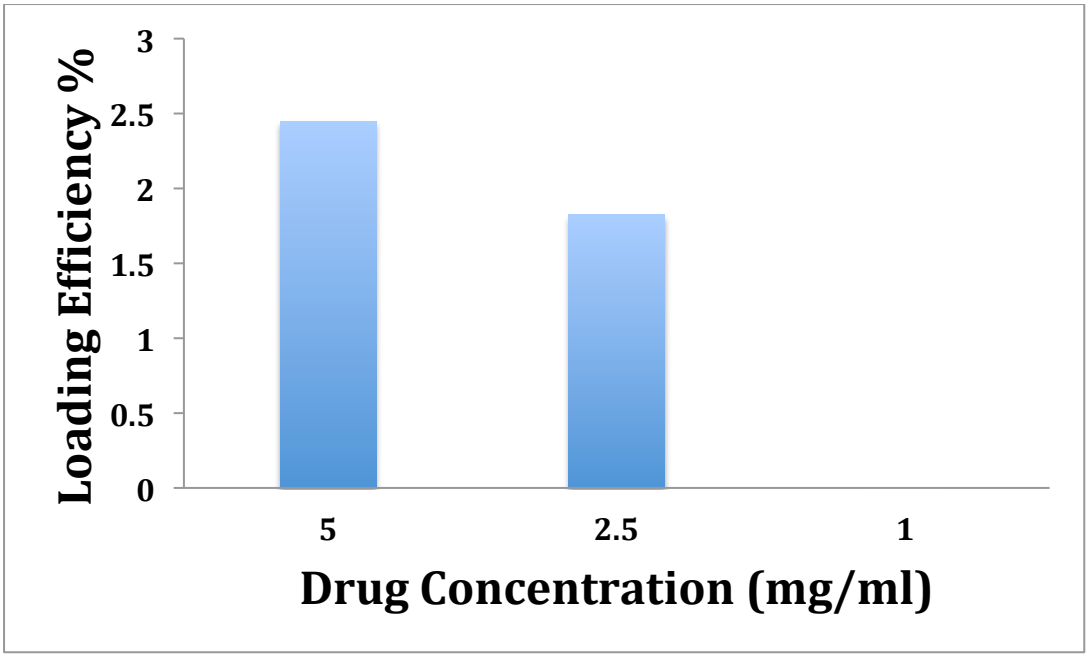

Figure 29. Loading efficiency as a fucntion of paracetamol cocnentration for 1 mg/ml of BSA Gold Nanoclusters

Loading efficiency increases with an increase in particle concentration. Although a linear relationship could be expected, the data does not corroborate such assumption. This can be attributed to the unknown conformation of the BSA-gold nanoclusters. Further more, From Fig 30 different L.E., 6% and 2.45%, can be observed for the same conditions, hence supporting the conformational assumption. It is unknown how many gold clusters are there on each molecule of BSA and whether if the molecule is extended or collapsed in itself.

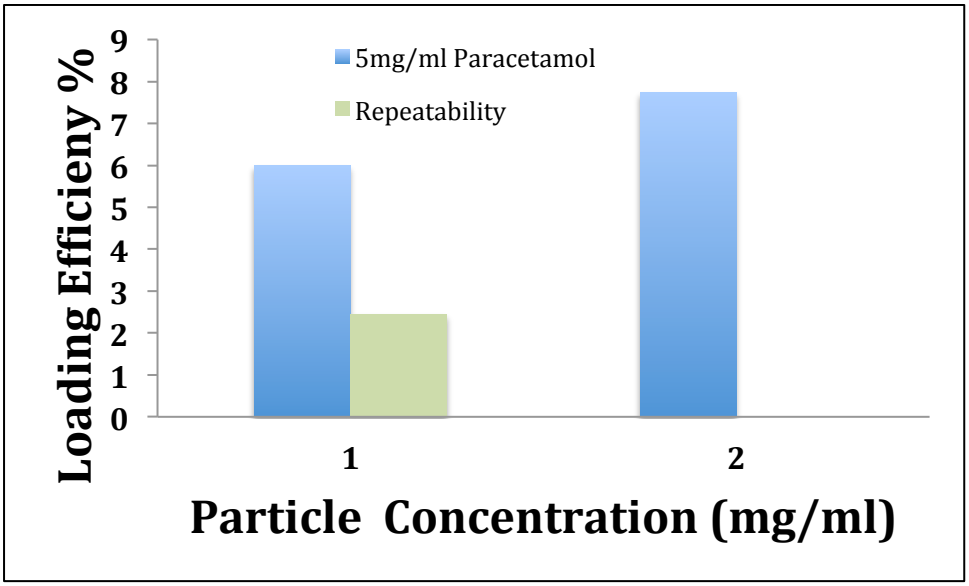

Figure 2. Loading efficiency of Fe@Ag as a function of particle concentration (blue). Reapeatability experiment (green)

Drug release

Drug release study was performed in two different mediums, water and phosphate buffer saline solution. From the fig… only an initial release of paracetamol from the NPs can be observed in both mediums. This initial release can be attributed to the release of paracetamol bound in the secondary site of BSA described by Sułkowski *et al*[37] under the assumption that this is a weak interaction (not covalent bonding) between paracetamol and BSA.

On the other hand the stagnant drug release observed for both experiments is due to the irreversible binding of paracetamol at the major binding site as stated by *Streeter et al.*[36] and *Hoffman et al*[13].

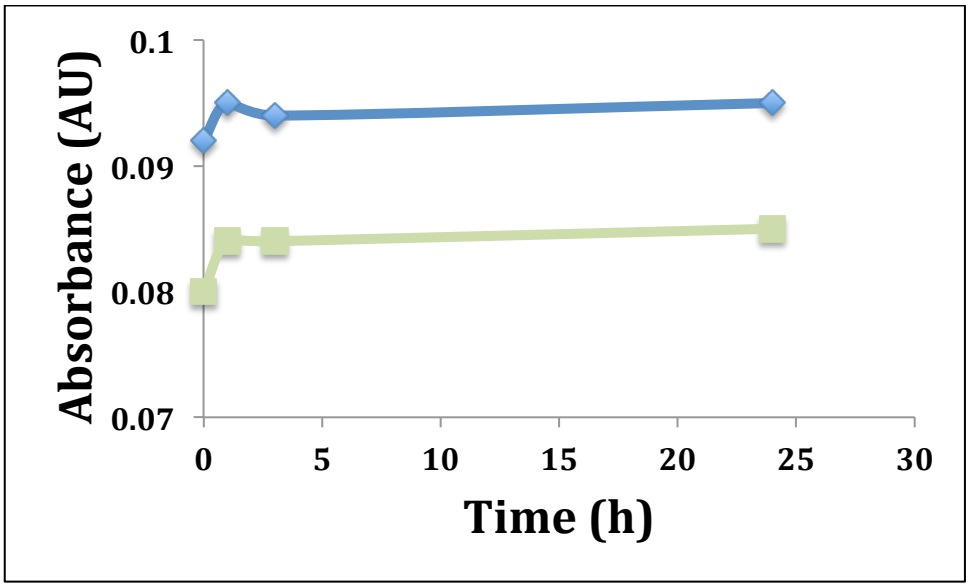

Figure 3. Drug release profile for paracetamol loaded Fe@Ag-BSA particles in water (blue) and phosphate buffer solution PBS (green).

The initial drug release in case of paracetamol-BSA can be considered diffusion controlled. To further increase drug release a different mechanism such as chemical controlled may be more suitbale, inducing the cleavage of the covalent bond previously discussed.

Conclusion

Effort has been given to advance the understanding of potential NPs, in this case core-shell NPs, in drug delivery applications. In the course of the thesis, a method for the synthesis of Fe@Ag core-shell NPs, has been adapted from *Caroll et al*[19] and modified to form a stable, monodisperse population of spherical NPs with an average size of 39nm. They are stable in polar solvents with a zeta potential of -26mV in aqueous medium, which is a well desired property for NPs that need to be retained long enough in circulation to reach the desired site of action.

The characterized NPs were tried to be coated with functional polymers PNIPAM and PLL. Successful coating showed that these NPs can be easily functionalized owing to the initial citrate coating that is easy to displace with other ligands and also enables electrostatic adsorption of charged polymers. Paracetamol, a standard drug, was tried to be loaded to these polymer coated NPs. PNIPAM coated NPs showed a higher loading of the drug owing to better electron density matching (assumed) as compared to PLL. Further studies with these systems were not carried out with an intent to achieve higher loading efficiencies.

BSA, a protein that also serves the function of a carrier molecule for various compounds, was chosen as the next molecule to understand its adsorption to Fe@Ag NPs. Two different methods were employed to adsorb the BSA onto the NPs. In one case, the BSA was mixed with the paracetamol, followed by its adsorption onto the NPs. While in the second case, the BSA was first adsorbed on the NPs, followed by incorporation of paracetamol. In the former case, all the available conformations of BSA could be exploited to bind the drug, whereby expecting a higher loading efficiency. In the latter case, BSA, upon binding to the NPs, loses some of its available sites for drug binding, leading to lower loading efficiencies. Although, the main aim was to avail of a high loading efficiency, difficulty to separate the free paracetamol from the BSA by centrifugation in the former case turned out to be a practical problem. Hence, subsequent studies were carried out using the later strategy. Therafter, the effect of particle concentration on loading efficiency was studied and it was observed that at

higher particle concentration, a high loading was achieved (ca 8.3%). This was attributed to the fact that high enough surface area was needed for the drug to bind to the NPs. At this point, it was observed, that the major driving force for adsorption was hydrophobic interactions between the drug and the BSA molecule.

To better understand these, modified BSA (Au nanoclusters) were used to study the loading of paracetamol. Upto 6% loading could be achieved using these modified BSA constructs. It might be interesting to study the effect of particle concentration in this case and to see if optimization of particle, drug concentrations can yield a high loading efficiency.

A couple of release experiments were performed to understand the release kinetics of paracetamol. However, it was observed that the release kinetics is extremely slow. Further enhancement of the release may be obtained by changing the release medium (varying pH, temperature) or by utilizing the modified BSA nanoclusters, which seem to efficient drug delivery vectors.

Results have proven that the main factor influencing drug loading is drug-carrier interactions and more specifically the nature of such interactions. The drug must have greater affinity toward the carrier than the surrounding environment, but not to great affinity hindering the main goal, drug delivery.

Future Work

The current study has focused on Fe@Ag NPs for the purpose of loading paracetamol (standard drug) and to understand the release kinetics of the same in physiological medium. Although the current results indicate a low release percentage of the drug, it would be interesting to vary the release conditions to see the effect on drug release. This can be achieved by varying the pH, increasing the temperature (which might cause change in conformation of the polymer or protein molecule, without disturbing their inherent properties) or by shifting to a completely new set of core shell particles with different functional coatings.

Although outside the present scope of the study, it might be interesting to understand what are the different mechanisms by which paracetamol binds to the NP constructs and what subtle changes can cause a rapid change in orientation of the molecules leading to release. This might prove beneficial to understand the release mechanism of the drug from such NP constructs.

To verify the loading and release capacities of the NPs, a simple experimental matrix comprising a more (than paracetamol) hydrophilic drug can be carried out. If similar release kinetics are obtained, interaction models between the drug and the carrier can be hypothesized to better understand the role of fundamental forces (Vanderwaal's, electrostatic, steric or hydrophobic) responsible for a high loading and yet a slow and non-efficient release. On the other hand, if a faster release kinetics is observed, it can be attributed simply to the fact that some drugs are better for some nanocarriers and vice versa.

Another interesting area of study could be to investigate the modified BSA (Au nanoclusters) in potential drug delivery. These novel materials are yet to be tested out for drug delivery applications. Their method of preparation is quite simple while a multitude of properties can be harvested from them, including optical detection, bioavailability, and prolonged circulation. These constructs could be loaded with different drugs to see if multi drug loading and release, effected by different external conditions can be achieved.

As is the case with related studies, a judicious choice of the nano-carrier and the drug forms the vital part of enhancing NP mediated loading and release.

1 A. K. Bajpai, Sandeep K. Shukla, Smitha Bhanu, and Sanjana Kankane, 'Responsive Polymers in Controlled Drug Delivery', *Progress in Polymer Science,* 33 (2008), 1088-118.
2 J. L. Burt, C. Gutiérrez-Wing, M. Miki-Yoshida, and M. José-Yacamán, 'Noble-Metal Nanoparticles Directly Conjugated to Globular Proteins', *Langmuir,* 20 (2004), 11778-83.
3 S. Cammas, K. Suzuki, C. Sone, Y. Sakurai, K. Kataoka, and T. Okano, 'Thermo-Responsive Polymer Nanoparticles with a Core-Shell Micelle Structure as Site-Specific Drug Carriers', *Journal of Controlled Release,* 48 (1997), 157-64.
4 Krishnendu Chatterjee, Sreerupa Sarkar, K. Jagajjanani Rao, and Santanu Paria, 'Core/Shell Nanoparticles in Biomedical Applications', *Advances in Colloid and Interface Science,* 209 (2014), 8-39.
5 Weiren Cheng, Liuqun Gu, Wei Ren, and Ye Liu, 'Stimuli-Responsive Polymers for Anti-Cancer Drug Delivery', *Materials Science and Engineering: C*.
6 Ashutosh Chilkoti, Matthew R. Dreher, Dan E. Meyer, and Drazen Raucher, 'Targeted Drug Delivery by Thermally Responsive Polymers', *Advanced Drug Delivery Reviews,* 54 (2002), 613-30.
7 Patrick Couvreur, and Christine Vauthier, 'Nanotechnology: Inteligent Desing to Treat Complex Disease', *Pharmaceutical Research* (2006).
8 Fabienne Danhier, Olivier Feron, and Véronique Préat, 'To Exploit the Tumor Microenvironment: Passive and Active Tumor Targeting of Nanocarriers for Anti-Cancer Drug Delivery', *Journal of Controlled Release,* 148 (2010), 135-46.
9 Prashant K. Deshmukh, Ketan P. Ramani, Saurabh S. Singh, Avinash R. Tekade, Vivekanand K. Chatap, Ganesh B. Patil, and Sanjay B. Bari, 'Stimuli-Sensitive Layer-by-Layer (Lbl) Self-Assembly Systems: Targeting and Biosensory Applications', *Journal of Controlled Release,* 166 (2013), 294-306.
10 Tennyson Doane, and Clemens Burda, 'Nanoparticle Mediated Non-Covalent Drug Delivery', *Advanced Drug Delivery Reviews* (2012), 607-21.
11 Hemda Baabur-Cohen Ela Markovsky, Anat Eldar-Boock, Liora Omer, Galia Tiram, Shiran Ferber, Paula Ofek, Dina Polyak, Anna Scomparin, Ronit Satchi-Fainaro, 'Administration, Distribution, Metabolism and Elimination of Polymer Therapeutics', *Journal of Controlled Release,* 161 (2012), 446-60.
12 L. G. Gómez-Mascaraque, R. Palao-Suay, and B. Vázquez, '12 - the Use of Smart Polymers in Medical Devices for Minimally Invasive Surgery, Diagnosis and Other Applications', in *Smart Polymers and Their Applications*, ed. by María Rosa Aguilar and Julio San Román (Woodhead Publishing, 2014), pp. 359-407.
13 Kurt-Jürgen Hoffmann, Anthony J. Streeter, Donald B. Axworthy, and Thomas A. Baillie, 'Structural Characterization of the Major Covalent

Adduct Formed in Vitro between Acetaminophen and Bovine Serum Albumin', *Chemico-Biological Interactions,* 53 (1985), 155-72.

14 Iain K. Moppett Jonathan N. Wilkinson, Jonathan G. Hardman, 'Modes of Drug Elimination', *Anaesthesia & Intensive Care Medicine,* 9 (2008), 362-65.

15 Anja Judefeind, and MelgardtM de Villiers, 'Drug Loading into and in Vitro Release from Nanosized Drug Delivery Systems', in *Nanotechnology in Drug Delivery*, ed. by MelgardtM de Villiers, Pornanong Aramwit and GlenS Kwon (Springer New York, 2009), pp. 129-62.

16 Clement Kleinstreuer, Emily Childress, and Andrew Kennedy, 'Chapter 10 - Targeted Drug Delivery: Multifunctional Nanoparticles and Direct Micro-Drug Delivery to Tumors', in *Transport in Biological Media*, ed. by Sid M. Becker and Andrey V. Kuznetsov (Boston: Elsevier, 2013), pp. 391-416.

17 Rainer Haag; Felix Kratz, 'Polymer Therapeutics: Concepts and Applications', *Medicinal Chemistry* (2006), 1198-215.

18 A. Kumari, S. K. Yadav, and S. C. Yadav, 'Biodegradable Polymeric Nanoparticles Based Drug Delivery Systems', *Colloids and Surfaces B: Biointerfaces,* 75 (2010), 1-18.

19 Daniel M. Hudgins Kyler J. Caroll, Steven Spurgeon, Kenneth M. Kemner, Bhoopesh Mishra, Maxim I. Boyanov, Lester W. Brown III, Mitra L. Taheri, Everett E. Carpenter, 'One-Pot Aqueous Synthesis of Fe and Ag Core/Shell Nanoparticles', *Chemistry of Materials,* 22 (2010), 6291-96.

20 Min-Young Lee, Sang-Jun Park, Kitae Park, Ki Su Kim, Hwiwon Lee, and Sei Kwang Hahn, 'Target-Specific Gene Silencing of Layer-by-Layer Assembled Gold–Cysteamine/Sirna/Pei/Ha Nanocomplex', *ACS Nano,* 5 (2011), 6138-47.

21 Baoshun Li, Jianjun Li, and Junwu Zhao, 'Silver Nanoclusters Emitting Weak Nir Fluorescence Biomineralized by Bsa', *Spectrochimica Acta Part A: Molecular and Biomolecular Spectroscopy*.

22 M. S. Maleki, O. Moradi, and S. Tahmasebi, 'Adsorption of Albumin by Gold Nanoparticles: Equilibrium and Thermodynamics Studies', *Arabian Journal of Chemistry*.

23 Geoffrey A. Ozin, André C. Arsenault, and Ludovico Cademartiri, *Nanochemistry: A Chemical Approach to Nanomaterials* (Cambridge: Royal Society of Chemistry, 2009), pp. 1 online resource (liii, 820 s.) : ill. (some col.), ports.

24 Jiří Smolík Pavel Moravec, Helmi Keskinen, Jyrki M. Mäkelä, Snejana Bakardjieva, Valeri V. Levdansky, 'Niox Nanoparticle Synthesis by Chemical Vapor Deposition from Nickel Acetylacetonate', *Materials Sciences ad Applications,* 2 (2010), 258-64.

25 Margaret A. Phillips; Martin L. Gran; Nicholas A. Peppas, 'Targeted Nanodelivery of Drugs and Diagnostics', *Nano Today* (2010), 143-59.

26 M. Rajan; V. Raj, 'Encapsulation, Characterisation and in-Vitro Release of Anti-Tuberculosis Drug Using Chitosan-Poly Ethylene Glycol Nanoparticles', *International Journal of Pharmacy and Pharmaceutical Sciences,* 4 (2012).

27 Aswathy Ravindran, Anupam Singh, Ashok M. Raichur, N. Chandrasekaran, and Amitava Mukherjee, 'Studies on Interaction of

Colloidal Ag Nanoparticles with Bovine Serum Albumin (Bsa)', *Colloids and Surfaces B: Biointerfaces,* 76 (2010), 32-37.

28 F. Reyes-Ortega, '3 - Ph-Responsive Polymers: Properties, Synthesis and Applications', in *Smart Polymers and Their Applications*, ed. by María Rosa Aguilar and Julio San Román (Woodhead Publishing, 2014), pp. 45-92.

29 D. Kashchiev; G.M van Rosmalen, 'Review: Nucleation in Solutions Revisited', 38 (2003), 555-74.

30 Dirk Schmaljohann, 'Thermo- and Ph-Responsive Polymers in Drug Delivery', *Advanced Drug Delivery Reviews* (2006), 1655-70.

31 Jonathan G. Hardman Shruti Chillistone, 'Modes of Drug Elimination and Bioactive Metabolites', *Anaesthesia & Intensive Care Medicine* (2014).

32 Richard B. Silverman, and Mark W. Holladay, 'Drug Metabolism', in *The Organic Chemistry of Drug Design and Drug Action*, ed. by Richard B. Silverman and Mark W. Holladay (Boston: Academic Press, 2014), pp. 357-422.

33 Kumaresh S. Soppimath, Tejraj M. Aminabhavi, Anandrao R. Kulkarni, and Walter E. Rudzinski, 'Biodegradable Polymeric Nanoparticles as Drug Delivery Devices', *Journal of Controlled Release,* 70 (2001), 1-20.

34 R. A. Sperling, and W. J. Parak, 'Surface Modification, Functionalization and Bioconjugation of Colloidal Inorganic Nanoparticles', *Philosophical Transactions of the Royal Society A: Mathematical, Physical and Engineering Sciences,* 368 (2010), 1333-83.

35 Robert P. Hesketh Stephanie Farell, Mariano J. Savelski, C. Stewart Slater 'Fundamentals, Design and Applications of Drug Delivery Systems', (2003).

36 A. J. Streeter, D. C. Dahlin, S. D. Nelson, and T. A. Baillie, 'The Covalent Binding of Acetaminophen to Protein. Evidence for Cysteine Residues as Major Sites of Arylation in Vitro', *Chemico-Biological Interactions,* 48 (1984), 349-66.

37 A. Sułkowska, B. Bojko, J. Równicka, and W. W. Sułkowski, 'Paracetamol and Cytarabine Binding Competition in High Affinity Binding Sites of Transporting Protein', *Journal of Molecular Structure,* 792–793 (2006), 249-56.

38 Conroy Sun, Jerry S. H. Lee, and Miqin Zhang, 'Magnetic Nanoparticles in Mr Imaging and Drug Delivery', *Advanced Drug Delivery Reviews,* 60 (2008), 1252-65.

39 Ranjita Misra Suphiya Parveen, Sanjeeb K. Sahoo, 'Nanoparticles: A Boon to Drug Delivery, Therapeutics, Diagnostics and Imaging', *Nanomedicine: Nanotechnology, Biology and Medicine,* 8 (2012), 147-66.

40 Mark T. Swihart, 'Vapor-Phase Synthesis of Nanoparticles', *Colloid and Interface Science,* 8 (2003), 127-33.

41 Nguyen T. K. Thanh, and Luke A. W. Green, 'Functionalisation of Nanoparticles for Biomedical Applications', *Nano Today,* 5 (2010), 213-30.

42 Melgardt M. Villiers, Pornanong Aramwit, and Glen S. Kwon, *Nanotechnology in Drug Delivery* (New York, NY: Springer New York, 2009), p.: v.: digital.

43 Li Yan, and Xianfeng Chen, 'Nanomaterials for Drug Delivery', in *Nanocrystalline Materials*, ed. by Sie-Chin Tjong (Oxford: Elsevier, 2014), pp. 221-68.
44 Weiyuan John Kao Yao Fu, 'Drug Release Kinectics and Transport Mechanisms of Non-Degradable and Degradable Polymeric Delivery Systems', *Expert Opinion Drug Delivery* (2010), 429-44.
45 James J. De Yoreo, and Peter G. Vekilov, 'Principles of Crystal Nucleation and Growth', *Reviews in Mineralogy & Geochemistry,* 54 (2003), 57-93.
46 D. H. Zhang, G. D. Li, J. X. Li, and J. S. Chen, 'One-Pot Synthesis of Ag-Fe(3)O(4) Nanocomposite: A Magnetically Recyclable and Efficient Catalyst for Epoxidation of Styrene', *Chemical Communications* (2008), 3414-16.
47 Hong-liang Zhang, Si-hui Wu, Yi Tao, Lin-quan Zang, and Zheng-quan Su, 'Preparation and Characterization of Water-Soluble Chitosan Nanoparticles as Protein Delivery System', *Journal of Nanomaterials,* 2010 (2010).